FINAL TECHNICAL REPORT

Grant
DE-EE0006958
High Performance Platinum Group Metal Free Membrane Electrode Assemblies through Control of Interfacial Processes

SUBMITTED BY

Proton Energy Systems d/b/a Proton OnSite
10 Technology Drive
Wallingford, Connecticut 06492

PRINCIPAL INVESTIGATOR

Kathy Ayers
203-678-2190
KAyers@ProtonOnsite.com

SUBMITTED TO

U. S. Department of Energy
Fuel Cell Technologies Office

David R. Peterson
David.Peterson@ee.doe.gov

REPORTING PERIOD

05/01/15 through 04/30/17

SUBMITTED ON

07 August 2017

Table of Contents

Acknowledgment: This material is based upon work supported by the U.S. Department of Energy's Office of Energy Efficiency and Renewable Energy (EERE) under the Fuel Cell Technologies Office (FCTO) under Award Number DE-EE0006958.

1. Executive Summary

Renewable sources of hydrogen are required to reduce the environmental impact of steam methane reforming, and can also contribute to zero emission vehicle deployment. Completely carbon-neutral fuel cell vehicles will require a renewable source of hydrogen fuel, such as water electrolysis powered by wind or solar. The DOE cost goals to produce renewable hydrogen are aggressively set to compete with existing fossil fuel-based infrastructure. Fuel cells and electrolyzers based on proton exchange membranes (PEMs) are well-known and continue to realize reductions in cost and improvements in performance. To meet DOE goals for renewable hydrogen production, and for growing energy markets, reductions in capital and operating costs are needed to justify electrolysis as a solution, particularly without incentives for zero carbon emissions.

To date, the only pathway with promise to achieve platinum group metal (PGM)-free electrode formulations in membrane-based electrolysis cells is utilization of anion exchange membranes (AEMs). The basic local environment of the membrane allows a range of stable transition metals (TM) and metal oxides to be utilized at high potential for catalysis. AEMs also enable the use of much less expensive flow field materials other than the titanium often used in PEM systems. At the same time, the solid-state electrolyte eliminates the need for corrosive liquid electrolytes such as concentrated potassium hydroxide and allows leveraging of high-performance membrane electrode assembly (MEA) technology. Proton has been exploring this technology with several collaborators since 2010 through an ARPA-E project in the GRIDS program and has made significant progress in understanding the limitations and potential of this AEM chemistry.

In the current project, catalyst, membrane, cell integration, and operating parameters were all investigated and critical performance issues were addressed in each area. On the catalyst side, Northeastern University worked to refine the inherent activity of non-PGM catalysts through adjustments in catalyst composition, focused on nickel alloys for both the hydrogen and oxygen electrodes. In parallel, University of New Mexico developed synthetic methods to create high surface area, self-supported catalysts through the Sacrificial Support Method (SSM) which were then combined with the Northeastern compositions. Membrane and ionomer work at Penn State focused on stabilization of polyphenylene oxide materials, including exploration of membrane reinforcement with materials supplied by Proton. Proton integrated the catalyst, membrane and ionomer materials into electrodes, and also tested different configurations of hydrophobic or hydrophilic gas diffusion layer materials and different electrolyte feed options.

The project resulted in completely PGM-free catalysts for both electrodes which passed durability testing at 500 mA/cm2 and maintained acceptable cell operating voltages. Membrane stability was also significantly improved, although this remains an area of needed focus. Proton continues to optimize electrode fabrication processes to achieve more consistent and uniform electrodes, and designed and built a new test stand with improved monitoring capabilities and circulation options. Surprisingly, feeding water or electrolyte on the cathode side of the cell, where the water is consumed, resulted in poor performance and increased degradation vs. anode feed. However, use of carbonate in the anode electrolyte continues to result in significantly improved cell performance vs. deionized water. This result is believed to be due in part to poor ion transfer at the ionomer-catalyst interface in the absence of supporting electrolyte. Overall, the program met all milestones and demonstrated continued improvement in stability and rate capability for AEM electrolyzers.

2. Project Goals/Objectives

The quantitative goal of this project was to produce a high-performance anion exchange membrane water electrolyzer (AEM-WE) completely free of platinum group metals (PGMs), which could operate for at least 500 hours with less than 50 microV/hour degradation, at 500 mA/cm^2. To achieve this goal, work focused on the optimization of electrocatalyst conductivity, with dispersion and utilization in the membrane electrode assembly (MEA) improved through refinement of deposition techniques. Critical factors were also explored with significant work undertaken by Northeastern University to further understand catalyst-membrane-ionomer interfaces and how they differ from liquid electrolyte. Water management and optimal cell operational parameters were established through the design, fabrication, and test of a new test station at Proton specific for AEM evaluation. Additionally, AEM material stability and robustness at high potentials and gas evolution conditions were advanced at Penn State.

Specifically, the effort was divided into the following sub-goals:

- Catalyst: Use sacrificial supports (such as silica, magnesia, clays etc) to synthesize un-supported mixed oxides or perovskite materials for the oxygen evolution reaction. This technique will be adopted for preparation of 10-25g batches of catalysts.
- Membrane and ionomer: Maintain the conductivity metrics demonstrated previously and improve the stability of ionomers and membrane by more than a factor of five, and scale up to +100g batches.
- Cell design: Tune hydrophobicity, porosity, and geometry of the gas diffusion layers and flow fields to optimize water management. Investigate alternate modes of water feed.

The work breakdown structure is shown in the figure below.

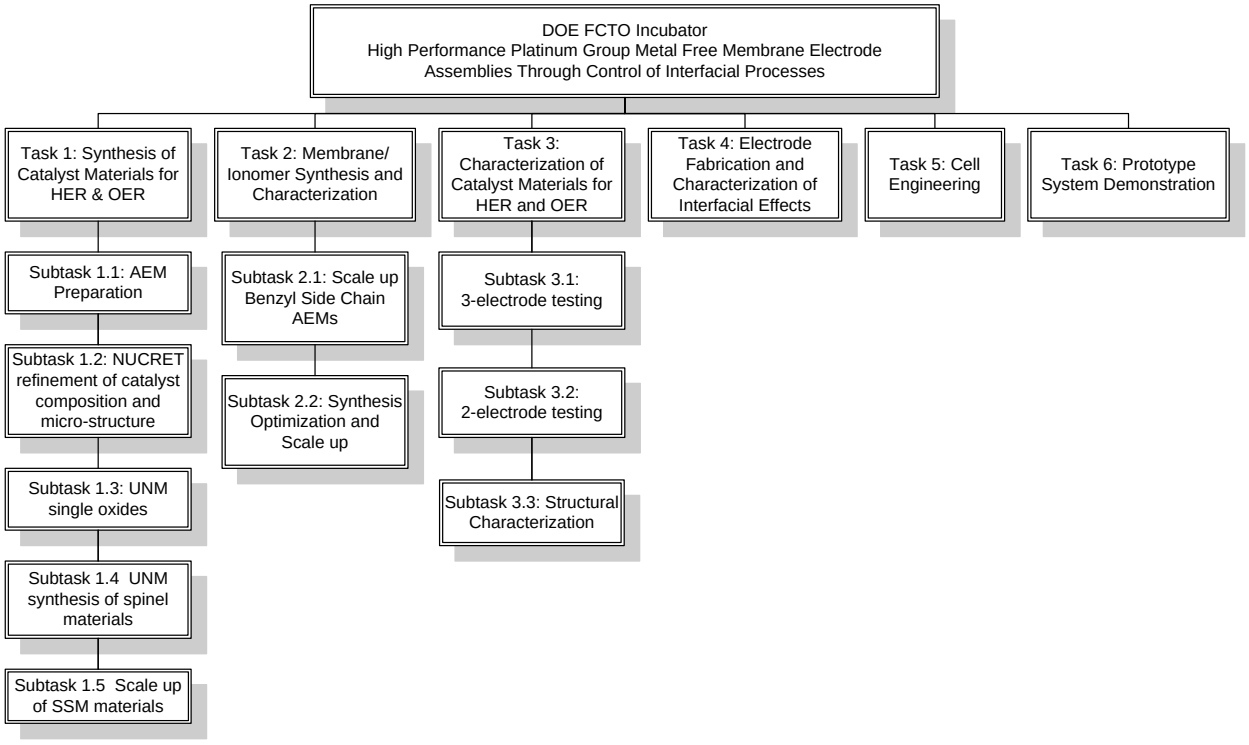

Figure 1: WBS for Overall Program

The following top-level milestones (**Table 1**) were used to measure progress and success during the 2-year program.

Milestone Summary Table				
Recipient Name:	Proton OnSite			
Project Title:	High Performance Platinum Group Metal Free Membrane Electrode Assemblies Through Control of Interfacial Processes			
Task # /Title	Type /#	Milestone/ Go –No Go Description	Milestone Verification Process	Q
1: Catalyst Synthesis	M1.1	**NUCRET:** Synthesize baseline Ni-Mo and Ni-Fe composite M/M_{Ox} materials in 0.5-1 g quantities and demonstrate structural equivalence to previous materials via XRD or other means.	Physical characterization: XRD, SEM to confirm structure, composition, and particle size	Q1 07/31/15 100%
1: Catalyst Synthesis	M1.2	**UNM**: Achieve single oxide catalyst material with similar half cell properties to IrO_2 (Surface area >20 $m^2\ g^{-1}$, electrical conductivity of 1 ohm-cm, onset potential of 1.4V)	Measure surface area by BET, electrical conductivity by 2-probe pressed pellet measurement, and onset potential in alkaline media via RRDE	Q2 10/31/15 100%
1: Catalyst Synthesis	M1.3	**NUCRET**: Identify 3 promising Ni/MeOx cathodes with HER overvoltage of less than 200 mV at 20 mA/cm^2; Identify 3 promising MTMO (Ni-Fe-Mo/Co) anodes with overvoltage of less than 320 mV at 20 mA/cm^2.	Electrochemical testing: RDE, 3-cell testing	Q3 1/31/16 100%
3: Catalyst Characterization	G/NG 1	**NUCRET:** Demonstrate operation of a non-PGM HER catalyst with standard PGM OER catalyst in an alkaline environment at 500 mA/cm^2, <2 V with liquid fuel in a three electrode flow through cell. Demonstrate operation of a non-PGM OER catalyst with standard PGM HER catalyst in an alkaline environment at 500 mA/cm^2, <2V with liquid fuel in a three electrode flow through cell.	3-electrode flow through cell testing with liquid fuel	Q4 4/30/16 100%
4: Electrode Fabrication and Characterization	M4.1	**Proton**: Integrate non-PGM catalyst with novel AEM materials and manufacture electrodes on catalyst coated membrane or gas diffusion layer with equivalent quality to baseline electrodes.	Pass standard acceptance procedures : lateral resistance and cross cell resistance within internal specification (<20 mohms for cross cell), visual inspection for no voids >3 mm in diameter, adhesion test score of 1 or 2	Q5 7/31/16 100%
2: Membrane Synthesis and Characterization	M2.1	**PSU**: Deliver 80-120 micron thick membrane materials with PPO benzyl side chain architecture and OH- conductivity > 25 mS/cm-1 in liquid water at room temperature for both membranes and cast ionomer for electrode optimization and cell testing.	30 membranes and 500 mL ionomer with PPO benzyl side chain, with confirmation of chemical structure measured by NMR and IEC data.	Q6 10/31/16 100%
1: Catalyst Synthesis	M1.4	**UNM**: Down select transition metal and precursor type for final non-pgm catalyst deliverable and scale up batch size to 10-25 g	The electronic conductivity within 5% of small-size batch; onset potential within 10% of small-size batch.	Q7 1/31/17 100%
6: Prototype Demonstration	M6.1	**Proton**: Demonstrate 500 hr of stable operation of a non-PGM (anode and cathode) alkaline membrane electrolysis cell at 500 mA/cm2, <2 V with less than 50 mV decay.	Electrolysis full cell electrochemical testing in 2-electrode configuration	Q8 4/30/17 100%

Table 1: Quarterly milestone table. OER = Oxygen evolution reaction; HER = Hydrogen evolution reaction. PPO = polyphenylene oxide

3. Accomplishments

Task 1.0 Synthesis of Catalyst Materials for HER & OER

HER and OER Synthesis of non-PGM Catalysts - NUCRET

In the following sections, the process for synthesis and down-selection of the best OER and HER catalysts will be discussed. Screening at the university labs was performed primarily in liquid electrolyte (0.1 M KOH), but all testing at Proton was done in MEA format.

OER catalysts

Development focused on the development and refinement of two OER catalysts: NiFe (9-1) /Raney-Ni and Ni-Fe-Co (8-1-1)/Raney-Ni. As shown in **Figure 2** below, the NiFeCo and NiFe blends both outperformed the IrOx standard OER catalyst and pure Raney Ni. Although the NiFeCo indicated better performance in RDE versus the NiFe, the Co salt is 3 times more costly than the Ni salts. Therefore, to scale up this OER catalyst cost-effectively, NiFe was chosen as the path forward.

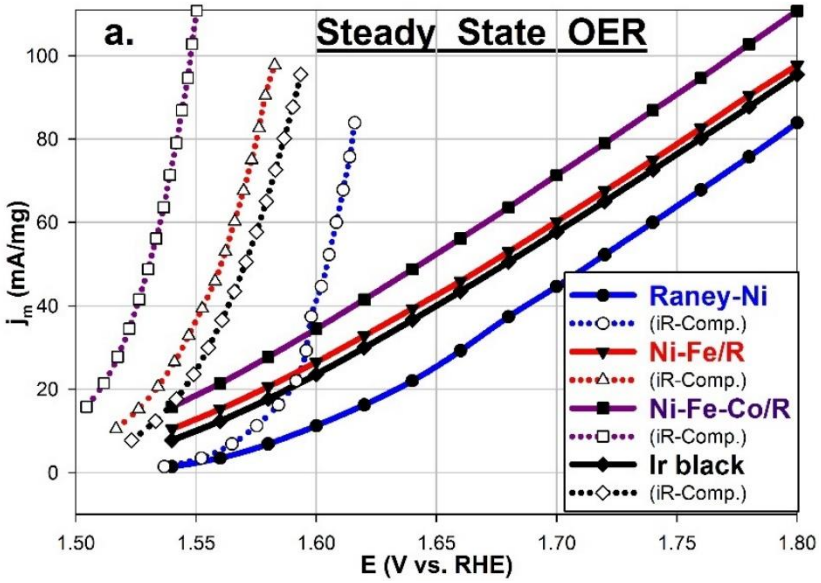

Figure 2: OER steady state of various Ni based materials on Raney-Ni compare to IrOx benchmark material and baseline support. Condition: Ar purged in 0.1M KOH, room temperature, 2500 rpm.

Further evaluation of the binary Ni-Fe MMO film indicated that annealing of the catalyst under argon increases OER activity relative to the non-annealed samples, shown below in **Figure 3, top**. Annealing tended to increase crystallinity as shown by the sharper peaks in the XRD pattern.

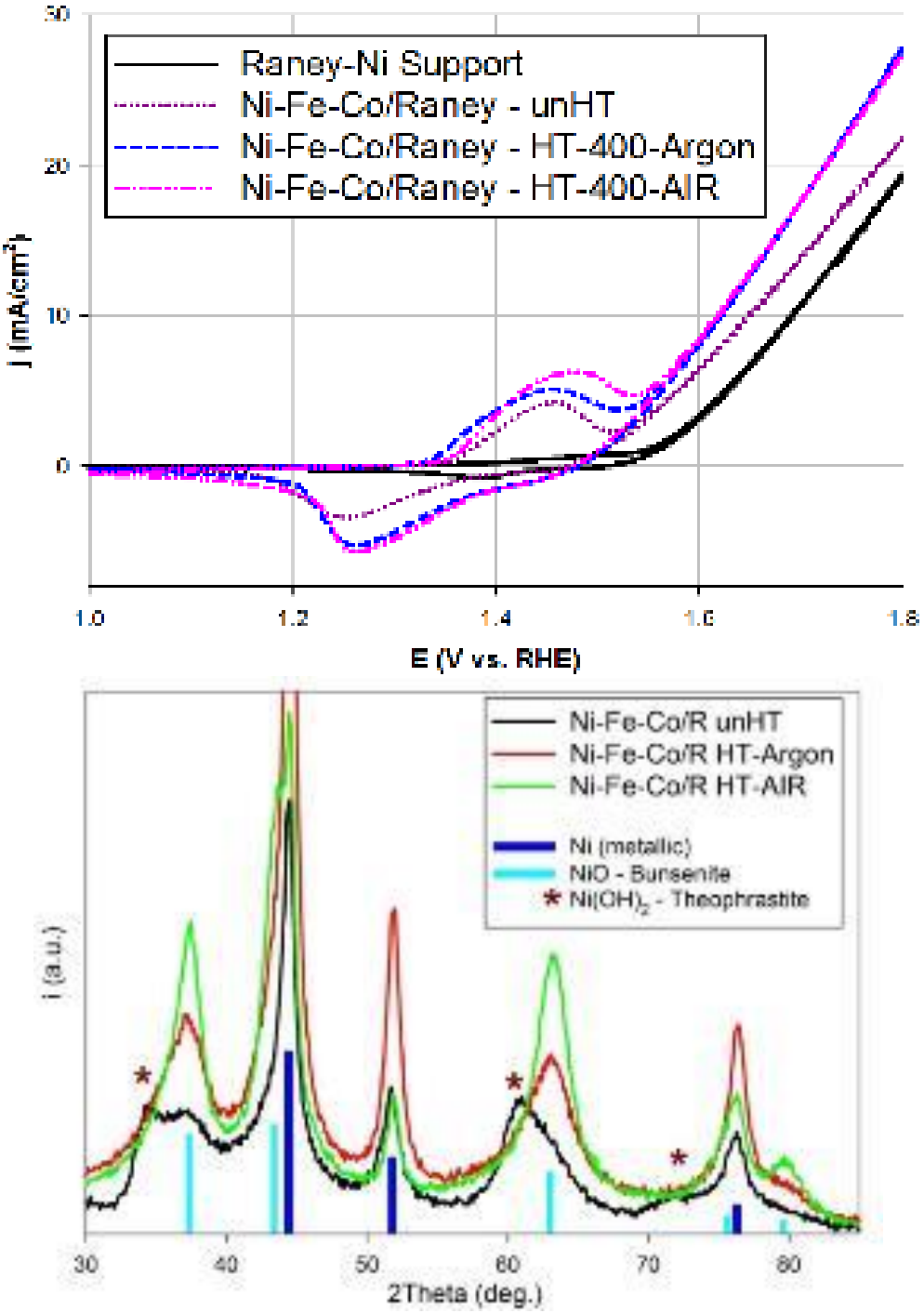

Figure 3: Top) CV data (20 mV/sec) showing HT-effects of Ni-Fe-Co on Raney-Ni support. Bottom) XRD data from Ni-Fe-Co/PANI-Raney

The **Q1 program milestone** was completed successfully with synthesis of baseline Ni-Mo and Ni-Fe composite M/MO_x materials in 0.5-1 g quantities. Structure, particle size, and composition were confirmed via XRD (**Figure 3**, **bottom**) and SEM (**Figure 4**).

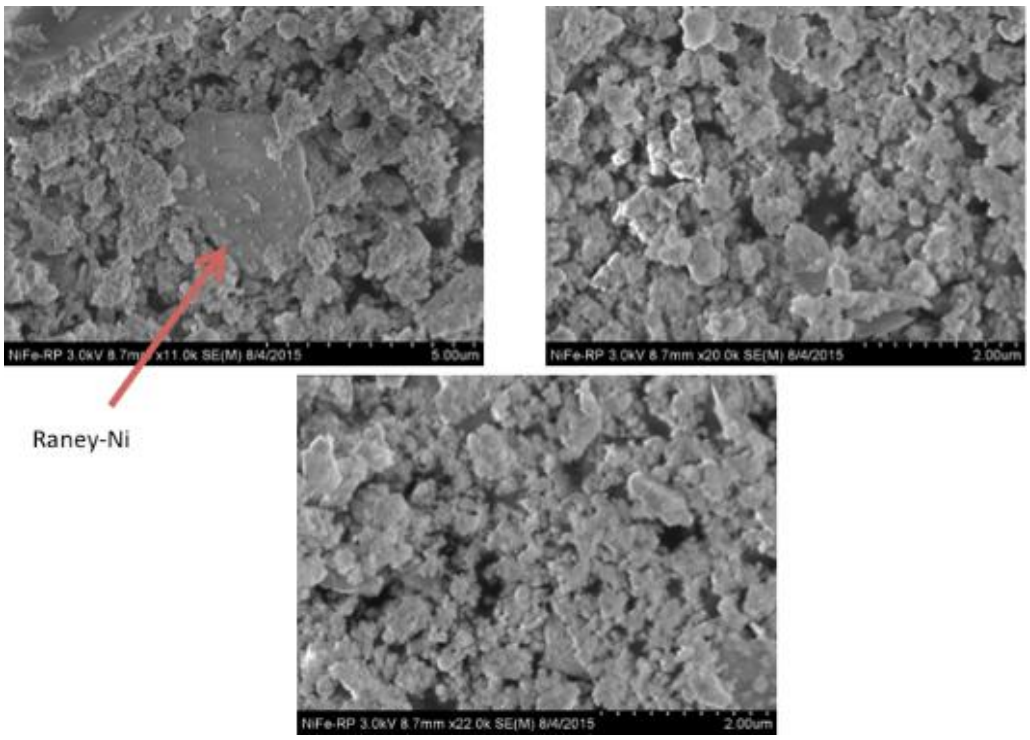

Figure 4: SEM images of Ni-Fe/Raney-Ni-PANI

The samples which successfully achieved the Q1 screening milestone targets were shipped to Proton for in-cell evaluation. These samples were successfully integrated in a 25cm^2 MEA, where they were operated against a PGM hydrogen electrode. Tokuyama A201 membrane was used with a 1wt% carbonate water feed with the cell operated at 50°C and 500 mA/cm^2. The test represented an evaluation of how well Proton could incorporate non-PGM catalysts into an electrode and to see if the bench results obtained at Northeastern in solution translated to in-cell performance. As shown in **Figure 5**, the NiFe/Raney material outperformed the PGM comparison by >300mV.

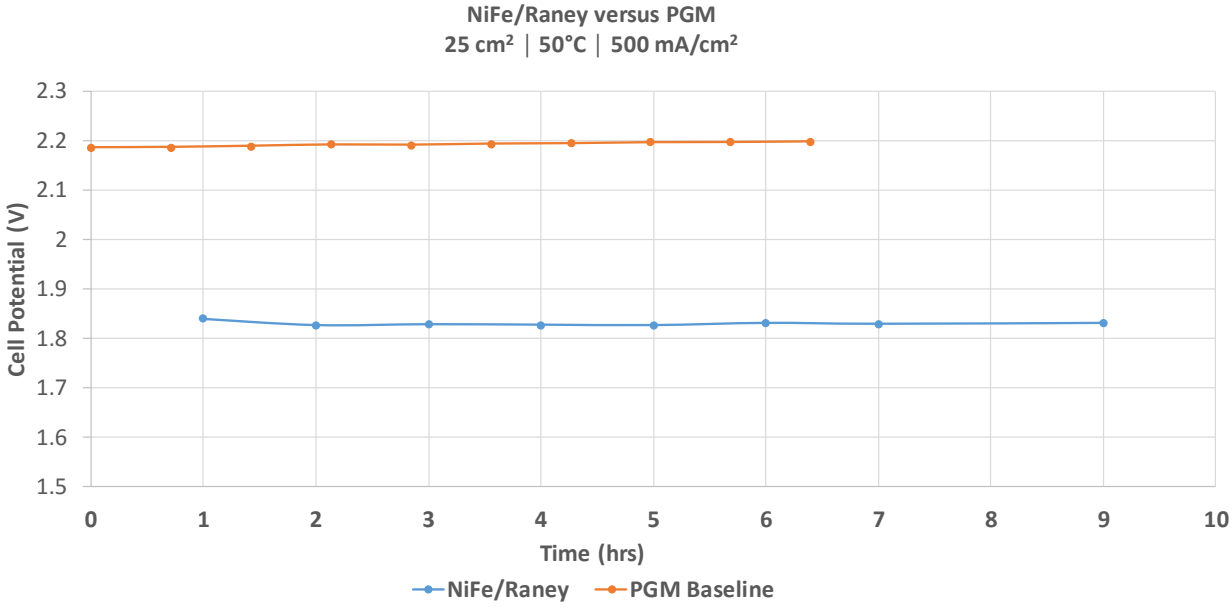

Figure 5: Comparison of NiFe/Raney against the PGM standard in steady-state testing

In addition to the significant improvement in electrical efficiency, the non-PGM test also exhibited stable performance over this short duration test. These results work to further support the successful development of a non-PGM OER catalyst at Northeastern University.

HER catalysts

During this project, a wide array of binary and ternary Ni-alloys and composite Ni/M_{Ox}/C (M_{Ox} = transition metal oxide) samples were explored, with Ni- -Cr_2O_3 providing performance rivalling that of state-of-the-art Ni-Mo. **Figure 6** below shows the steady state HER performance of the current state of the art Ni-Mo/C sample compared to the Ni-Cr/C and the Pt black benchmark.

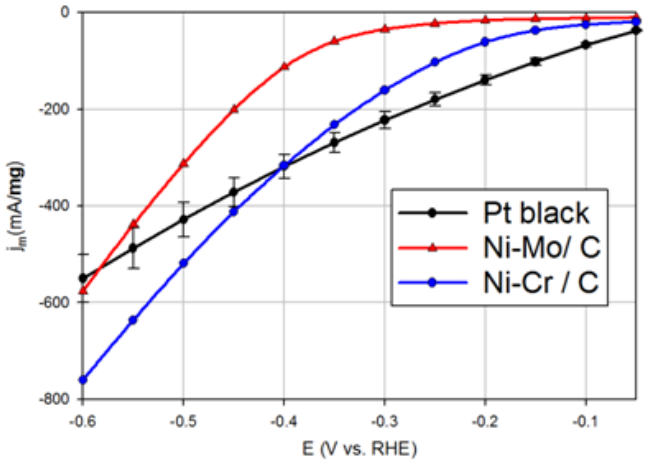

Figure 6: HER steady state that tested at condition: Ar purged in 0.1M KOH, 50°C, 2500 rpm

A significant stepping stone in the catalyst development was achieving the **Q3 milestone** by the NiFe/Raney and NiCr/C catalysts. Meeting these targets demonstrated successful synthesis of non-PGM catalysts that approach or exceed overpotential values typical of PGM materials. Supporting evidence for the milestone is shown below in the RDE testing conducted on 60% Ni-Cr/C and Ni-Mo for HER shown in **Figure 7**.

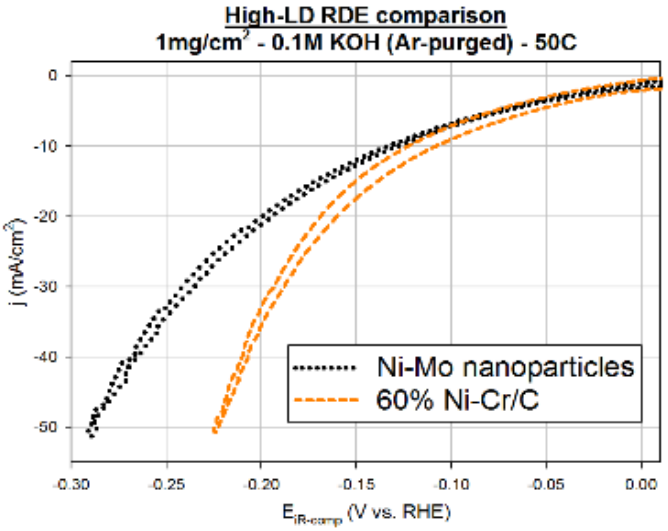

Figure 7: CV data (50 mV/sec), 1 mg/cm^2 catalyst loading, tested in Ar-purged 0.1M KOH at room temp (23°C), 3600 rpm, AS-4 binder

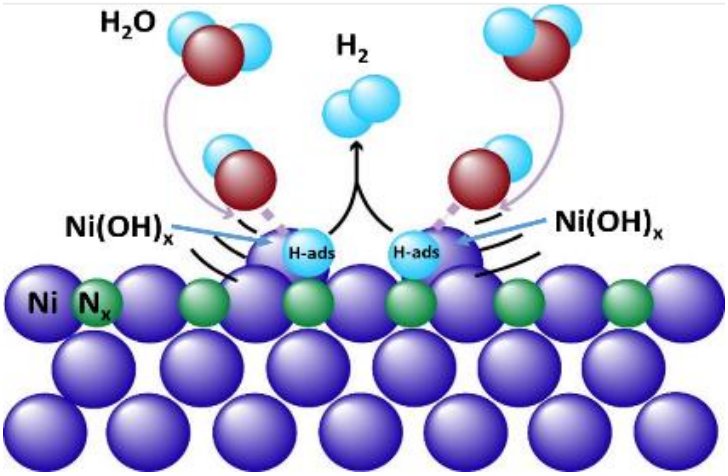

Figure 8: Proposed HER mechanisms of newly developed NiNx/C

SEM images show that the Ni-cupferron (1-2)/C catalyst exhibits fine particles of metals grown on the carbon support as seen in low magnification (**Figure 9**).

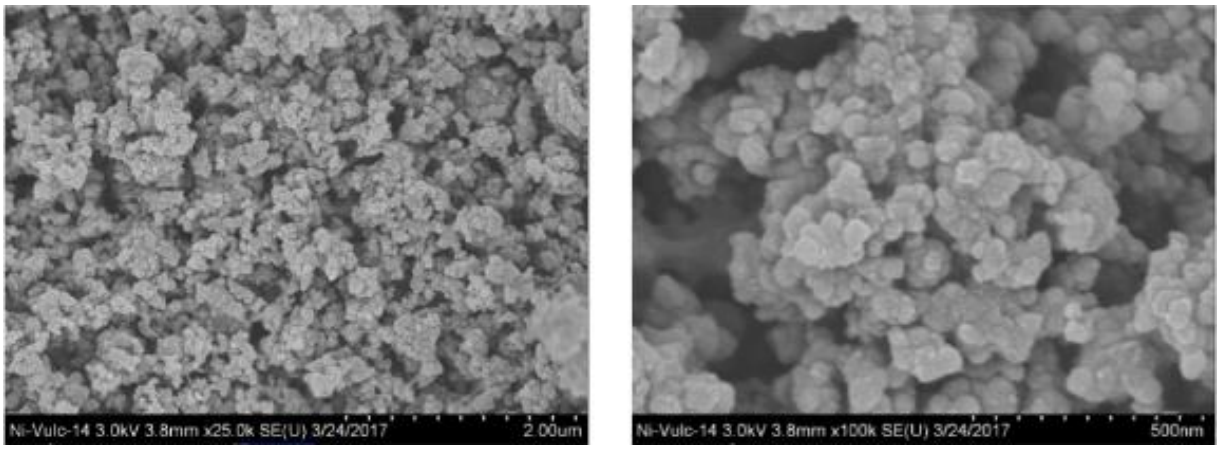

Figure 9: SEM images of 40% Ni-cupferron (1-2)/C

Evaluation through XRD (**Figure 10**) indicated that the composition only contained the nickel metal phase with no significant differences in the crystallite size.

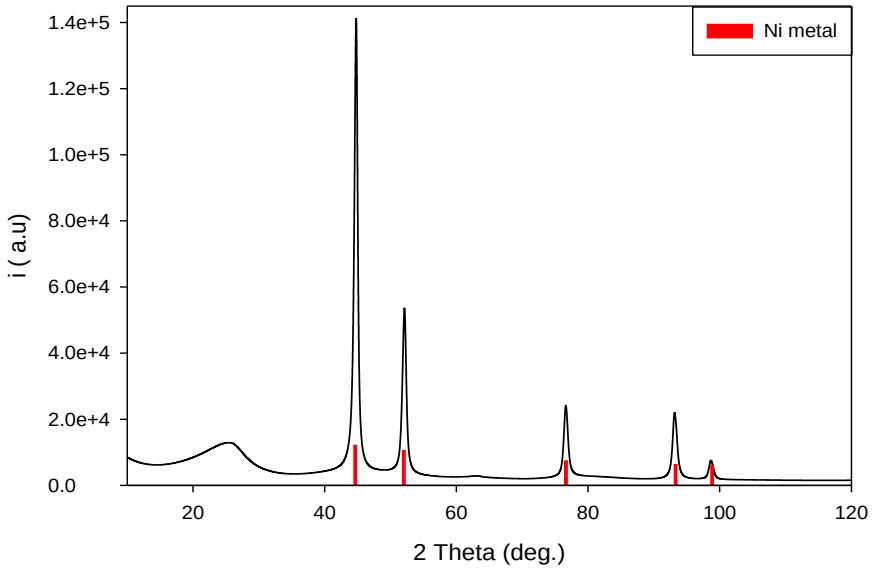

Figure 10: XRD pattern of 40% Ni-cupferron/C

Under RDE testing conditions (**Figure 11**), the HER activity of both NiCr/V and NiNx/C behaved essentially the same. Full cell testing of NiNx/C with A201 and a PGM OER electrode showed much higher performance as well as durability and was downselected as part of the **Q7 milestone (Figure 12)**. Theses downselected catalysts would feed directly into the final program milestone, Q8, which is discussed later in Task 6 of this report.

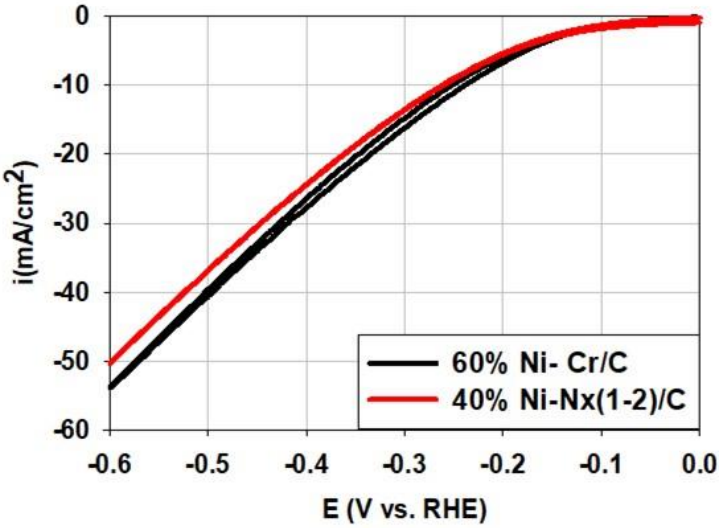

Figure 11: RDE testing

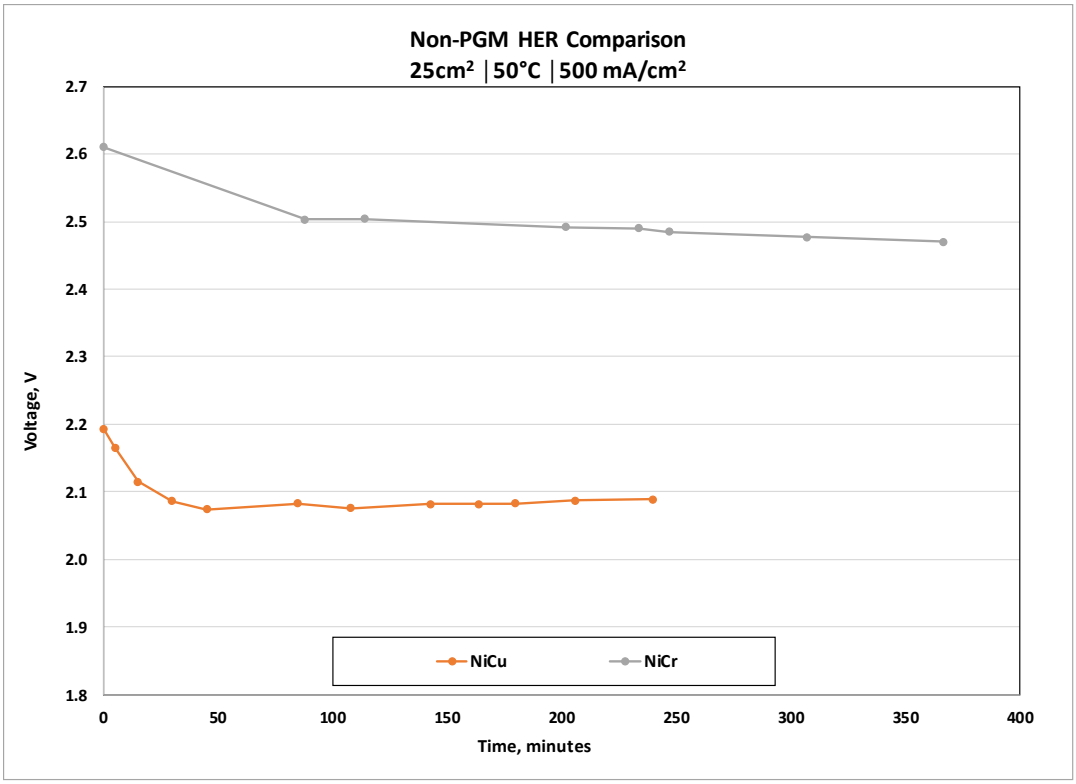

Figure 12: Operational comparison of the NiCr/C and NiNx/C HER catalysts

Sacrificial Support Method - UNM

In parallel to catalyst composition refinement at Northeastern, University of New Mexico treated catalysts with the Sacrificial Support Method (SSM) to achieve high surface area (20m^2 g^{-1} and more) and small particle size (smaller than 40nm). Initially NiO was used as a model compound to develop parameters for subsequent catalysts from Northeastern. Of the modifications evaluated, two methods were successful in exceeding the target with surface area of >50 m^2g^{-1} and were the result of incorporating different types of silica to influence the morphology. Details are described in the following section for the methods that were down-selected.

Synthetic details

SSM-2

In this modification, a hard template (silica) was selected, vs. a previous attempt with a support that melted too early to maintain the structure. 10g of L90 silica and 20g of nickel nitrate were mixed in a porcelain crucible and placed into the box furnace. The temperature was increased to 100 °C and held for 30min, after which temperature was increased at 5 °C/min until 250 °C was reached and then held again for 30min. Following the same ramped approach, temperature was then increased to 450 °C and held for 2h. The silica was removed by rinsing with a 7M KOH solution, followed by washing and drying the material.

The final material was found to have substantially less density compared to the SSM-1 and was easily dispersed by grinding. SEM analysis of the synthesized sample is shown on **Figure 13**. It can be clearly seen that the material has a well-developed porous structure with particles on the level of 20-35nm. BET analysis for this material revealed that surface area is close to 50m^2 g^{-1}, passing the Q2 milestone.

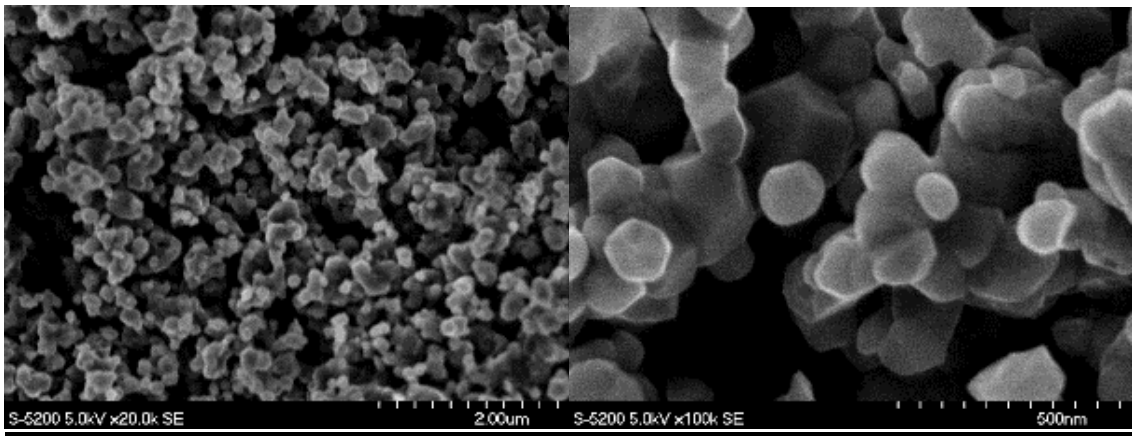

Figure 13. SEM images of NiO OER catalysts synthesized by SSM-2

SSM-3

In the third modification of the SSM approach, silica with increased surface area (SA) was selected as the template. L90 silica has a SA of $90m^2\ g^{-1}$, while EH5 has $400m^2\ g^{-1}$. The balance of the process was the same as or SSM-2. SEM analysis of synthesized sample is shown on **Figure 14**. The porous structure is similar to SSM-2 but BET surface area is close to $60m^2\ g^{-1}$. The success with this synthesis technique provided another option for the modified SSM approach.

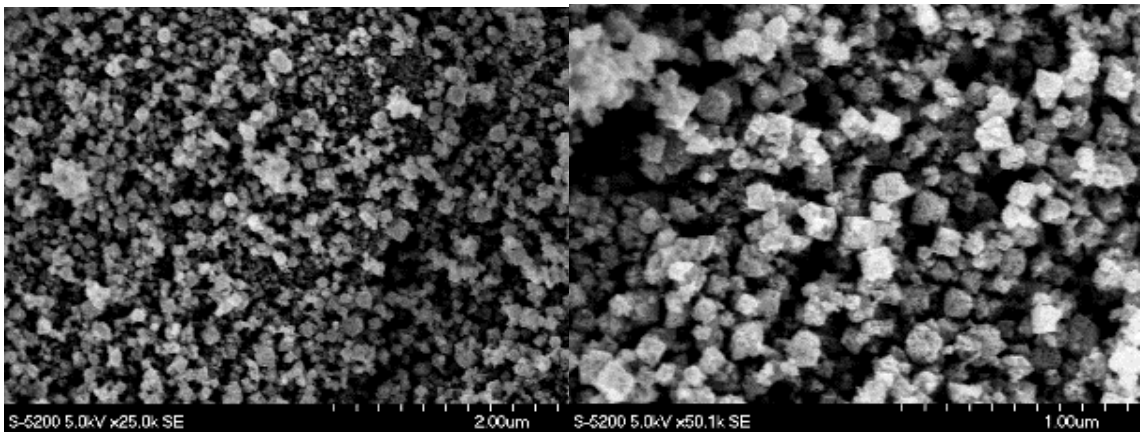

Figure 14: SEM images of NiO OER catalysts synthesized by SSM-3

Conductivity data

After using NiO as a model compound to develop the SSM technique used in this project, materials were synthesized by SSM based on the Northeastern compositions and were tested for electrical conductivity using a 2 pt probe set-up (**Table 2**). In order to measure the bulk conductivity, catalysts were pressed inside a Teflon cylinder.

	Conductivity [S/cm]	Onset Potential [V] vs RHE
NiMoCr	6.7	1.51
NiMoCo-311	2.92	1.51
NiMoCo-Scaled up	3.48	1.51
IrOx reference	0.0102	1.43

Table 2. Results of conductivity tests

Electrochemically the synthesized materials were active towards OER and on-set potential was only 80mV off the reference commercial IrO_x (**Figure 15**). These results are not quite as good as those observed with the original Northeastern catalysts. The difference in performance is believed to be related to the lower through plane conductivity of the low-loaded catalyst layer and lower electronic conductivity of the catalyst itself.

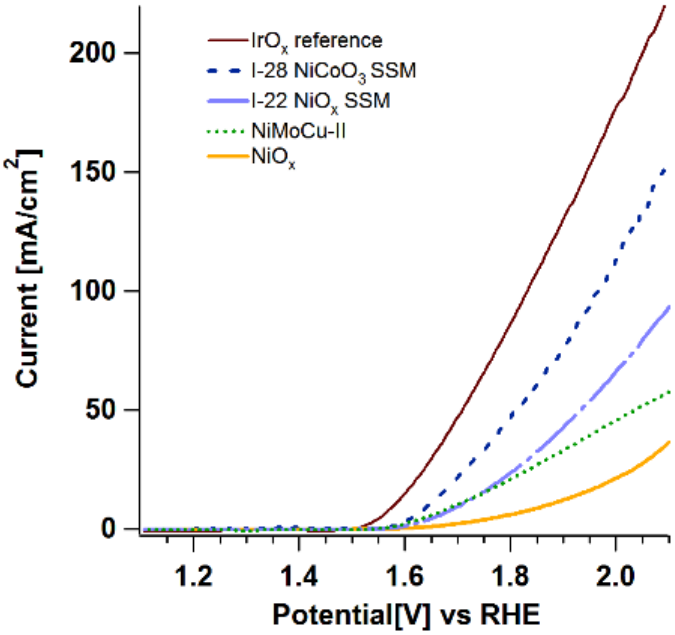

Figure 15: OER performance of electrocatalysts prepared by SSM and commercial IrO_x

UNM performed an initial scale up of NiMoCo catalyst to 5 grams. It was found that performance of scaled up materials was slightly higher than smaller batches, which can be explained by better heat/mass transfer in larger furnaces (**Figure 16**).

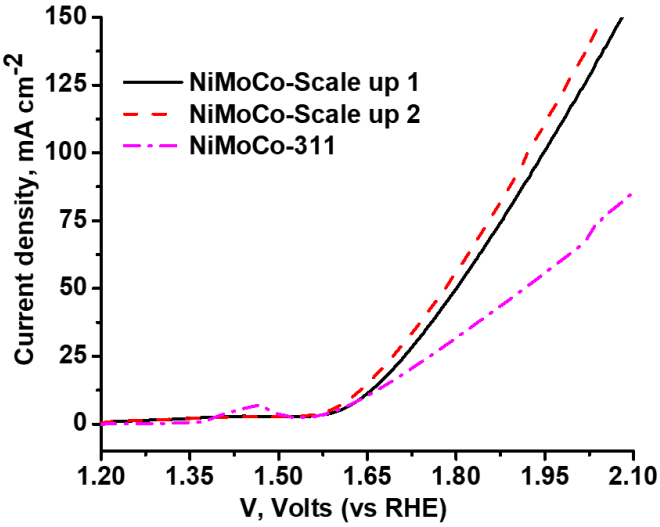

Figure 16: OER performance of scaled up NiMoCo electrocatalysts prepared by SSM

Technology Transfer – Northeastern and UNM

Leveraging the work between both University partners, the methodology of the SSM process and non-PGM compositions from Northeastern, a higher surface area support constituting Raney Ni was also fabricated using the University of New Mexico Si templating approach (sacrificial support method (SSM)). It was not clear from the CV data (**Figure 17**) whether the SSM samples havd higher activity than the Raney support. However, the steady-state data (**Figure 18)** suggests that this is the case. The ohmic resistances for 40% Ni-Fe-Co/Raney-PANI and Ni-Fe-Co/SiO_2 in 7 M KOH at 23ºC are 43 Ohm and 39 Ohm, respectively, while 35 Ohm was observed for the Ni-Fe-Co/SiO_2 in 7 M KOH at 80ºC.

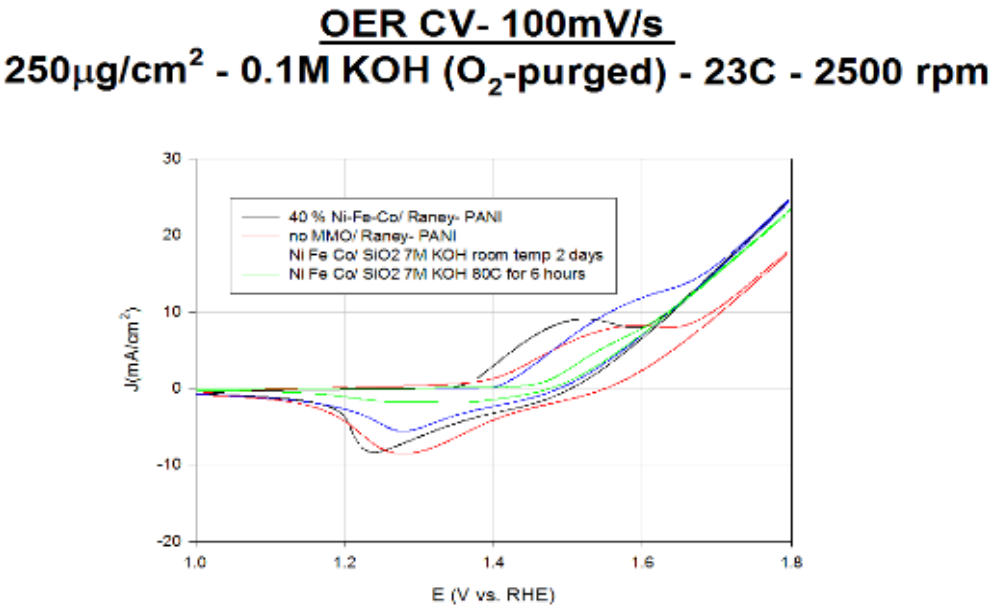

Figure 17: CV data (100 mV/sec), 250 ug/cm^2 catalyst loading, tested in O_2-purged 0.1M KOH at room temp (~23°C), 2500 rpm, Nafion binder.

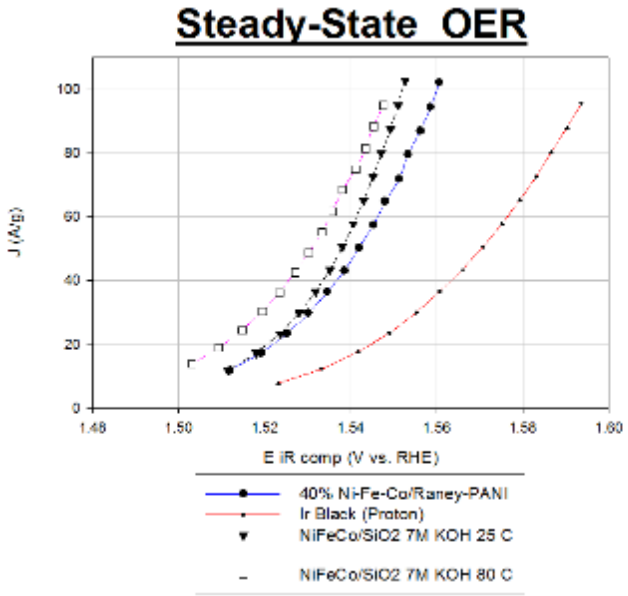

Figure 18: CV data (20 mV/sec), 250 ug/cm^2 catalyst loading, tested in O_2-purged 0.1M KOH at room temp (~25°C), 2500 rpm, and Nafion binder.

SEM images suggest the SSM samples mentioned above have “coral like” morphology, resulting in very high surface area (**Figure 19)**.

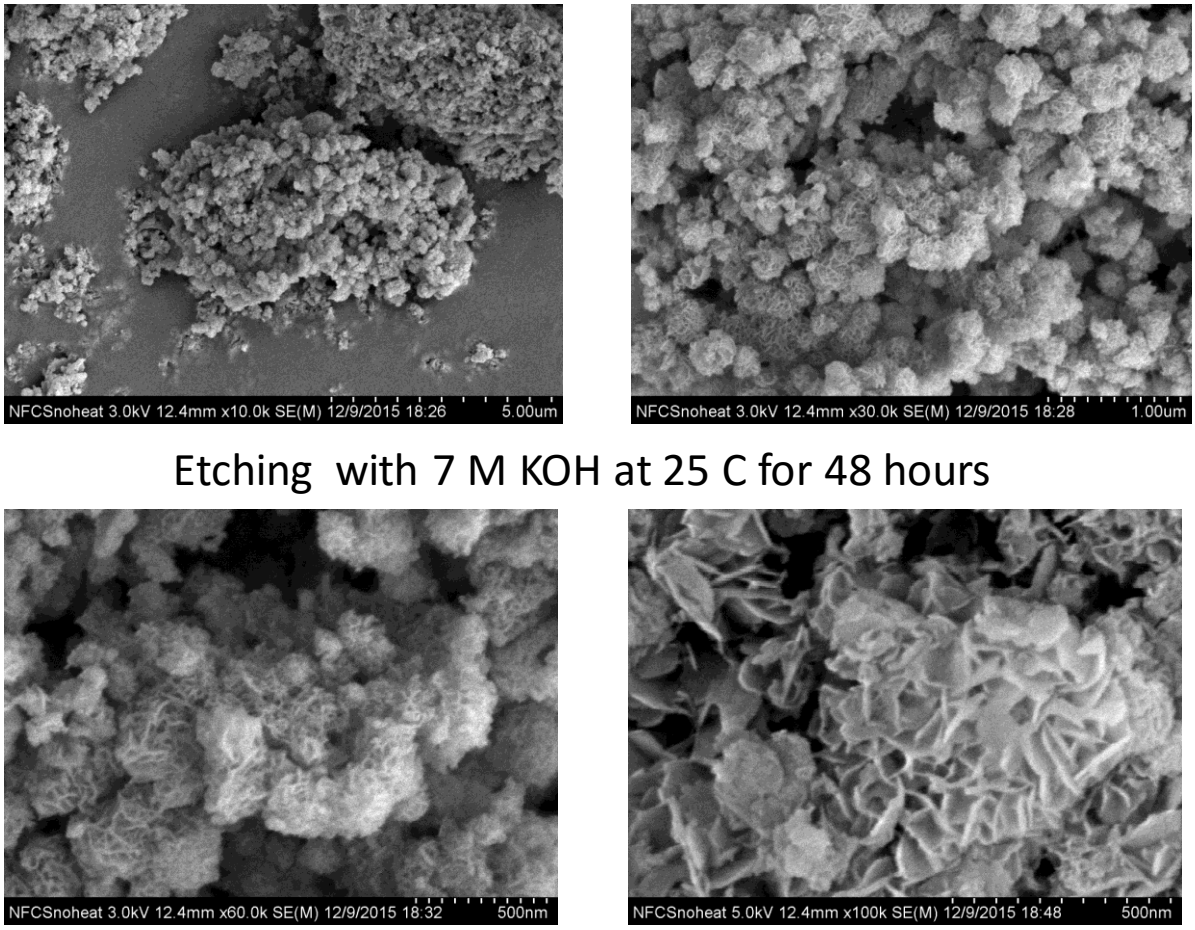

Figure 19: SEM image of Ni-Fe-Co/SiO_2 after heat treated in air at 550ºC and etched

With these results, Northeastern University was able to meet or exceed milestone performance targets on several different formulations of both the HER and OER catalysts as verified by electrochemical performance measurements. Additionally, through collaborative work with the University of New Mexico, the SSM process was transferred and successfully duplicated at Northeastern University.

Conclusions

The UNM team successfully modified SSM for synthesis of unsupported ternary compounds from the Ni-M_1-M_2 family. It was found that using different precursors, silica types, heat treatment conditions can control such important parameters as: particle size, phase purity, electrical conductivity, and surface area. More than 20 catalysts were synthesized and their OER activity was screened by RDE method. During initial screening, the Ni-Mo-Co catalysts were found to be promising and several iterations were made in order to increase their OER activity. The largest effect was the ratio between Mo and Co in these materials and finally NiMoCo-311 catalyst was selected for tests performed at Proton OnSite. UNM performed an initial scaling up effort which produced 5 g of NiMoCo-311 catalyst with activity similar or even larger compared to small batches.

Task 2.0 Membrane/Ionomer Synthesis and Characterization

Technical Approach

Penn State has shown that polyphenylene oxide (PPO) is a highly stable backbone for AEMs due to the absence of electron withdrawing groups in the main chain. These side chain benzyl dimethylalkyl ammonium polymers are capable of being produced in 100s of grams (**structure on left in Figure 0**). New work has shown that cation spacer polymers (**structure on right, Figure 20**) have 5-10 times greater hydroxide stability than the side chain benzyl-linked cation materials. The cation spacer dimethyldialkyl ammonium PPOs were targeted as next-generation ionomer and membrane materials with high stability. Small-scale work indicates that spacing the ammonium group away from the ring decreases benzyl attack, the predominant mechanism of cation degradation. Penn State was able to synthesize these polymers for use in ionomer solutions and membrane materials and provide samples to the project partners for operational experimentation. Ex-situ stability results were compared to in-situ stability to learn more about the degradation mechanisms occurring in the operating cell.

Side chain benzyl dimethylalkyl ammonium *Cation spacer dimethyldialkyl ammonium*

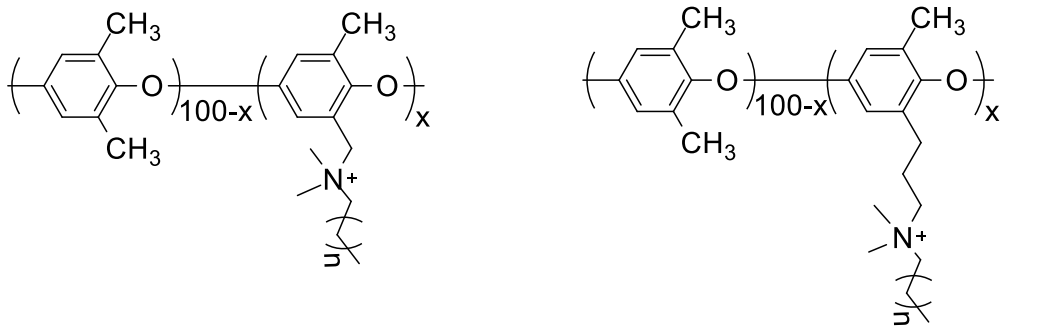

Figure 20: (left) Alkyl side chain benzyl dimethylalkyl ammonium PPO-based anion exchange polymers and (right) Cation spacer PPO polymer with dimethyldialkyl ammonium cations.

Over the course of the project, membranes and ionomer solutions of quaternary ammonium PPO AEMs were shipped to Proton for bench-top characterization and in-cell electrochemical testing. The samples provided by PSU were based on benzyltrimethyl ammonium (BTMA) cations. Water content and dimensional stability measurements were collected and provided to PSU to guide sample iteration.

Ionomer synthesis

Penn State's goal in this project was to produce large-scale, stable anion exchange membranes (AEMs) that showed sufficient performance to meet the device metrics. Large-scale synthesis of brominated poly(2,6-dimethyl-1,4-phyneylene oxide) was performed on the 1 kg scale to serve as a precursor for PPO-based AEMs based on traditional benzyltrimethyl ammonium cations, alkyl side chain cations, and multi-cation side chains, **Figure 21**. In device testing, these uncrosslinked samples proved to have insufficient stability and significant "erosion" of the membrane active area was observed in less than 10 hours of alkaline membrane electrolyzer device testing (**Figure 22**). Additionally, these uncrosslinked AEMs were difficult to process into membrane electrode assemblies (MEAs) due to their deformation under solvent and electrode pressing conditions.

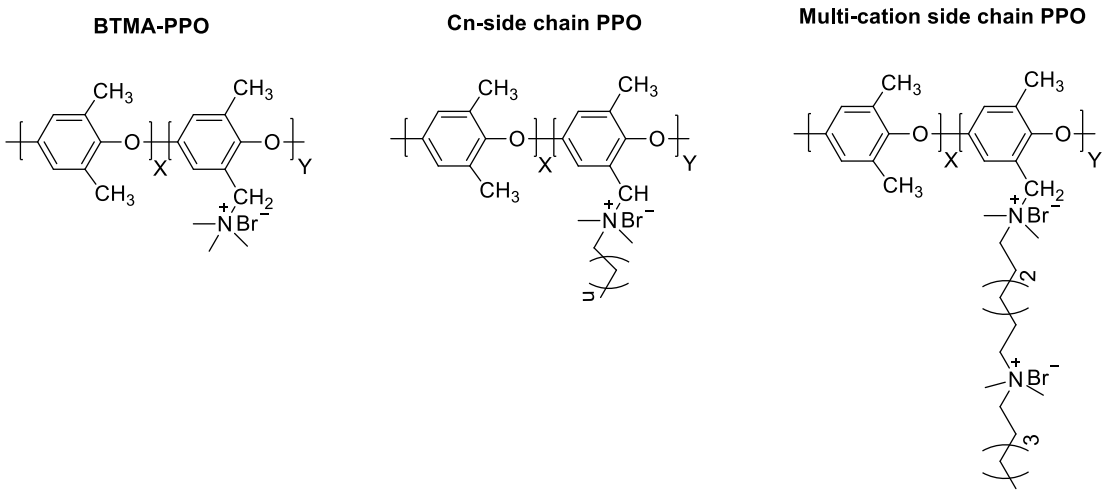

Figure 21: Initial, uncrosslinked QA-PPO samples based on different cations

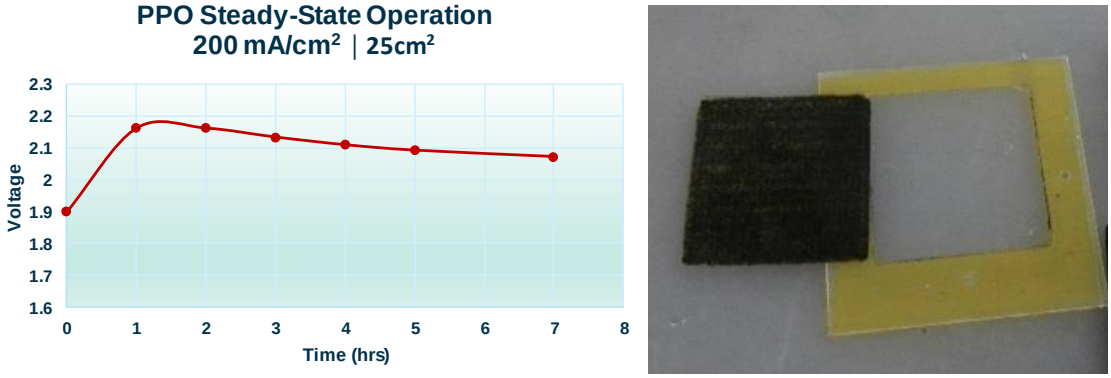

Figure 22: Steady-state data (left) and failed MEA (right) active area from solvent degradation

Testing was conducted on individual samples, where they were each exposed to a solvent or ionomer containing a solvent to assess the sensitivity (**Figure 23**).

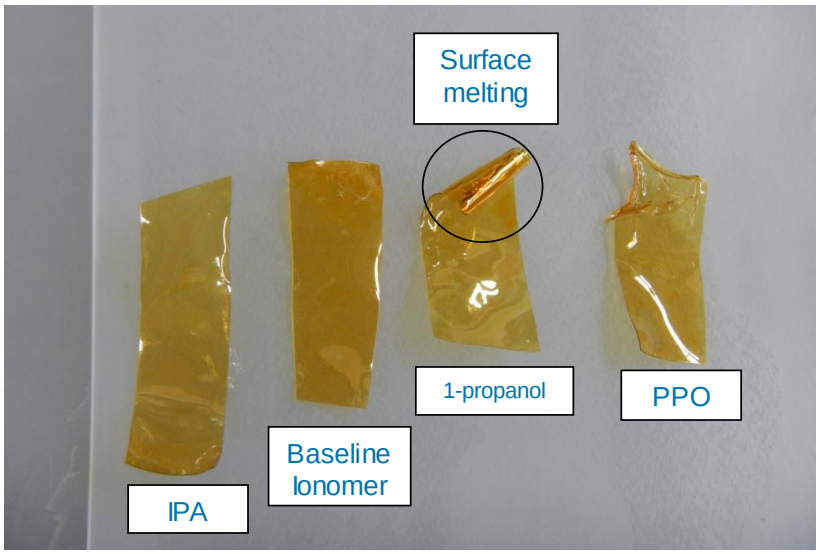

Figure 23: Membrane results after solvent exposure

To increase mechanical robustness of the membranes, Penn State fabricated crosslinked PPO membranes with the chemical structure shown in **Figure 24**. These membranes also incorporate C6 pendant alkyl chains on the cations, which have been observed to increase hydroxide stability. The water uptake and IEC properties of the crosslinked membranes are shown in **Table 3** below.

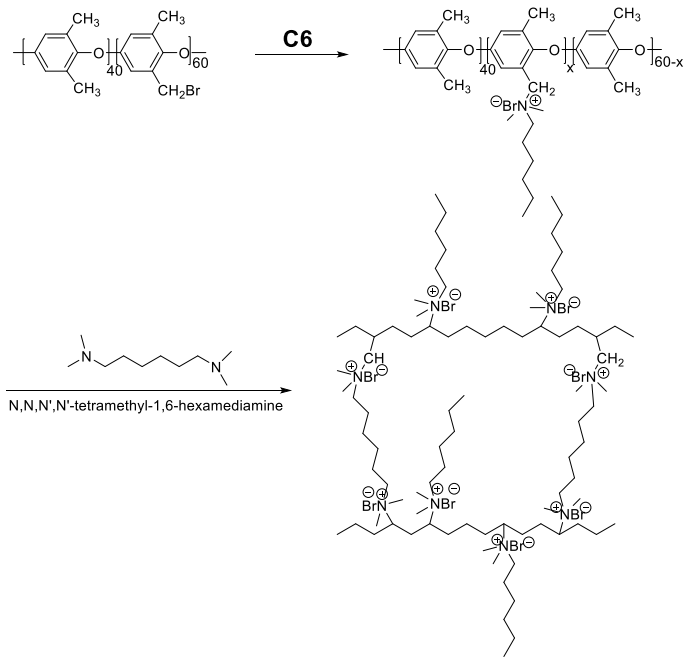

Figure 24: C6 crosslinking of PPO-based AEMs with a mixture of N,N-dimethylhexamine and N,N,N',N'-tetramethyl-1,6-hexamediamine

Sample	Water uptake (wt.)%(Cl^-)	IEC (meq./g)(Cl^-)	Water uptake (wt.)%(OH^-)	Water uptake (wt.)%(HCO_3^-)
X27Y33	33 ± 1	2.94	59 ± 2	40 ± 1
Commercial	38	1.8		

Table 3: Properties of crosslinked AEMs. Xx represents the total of number of Br groups functionalized with N,N-dimethylhexamine. Yy represents the total of number of Br groups functionalized with N,N,N',N'-tetramethyl-1,6-hexamediamine

The crosslinked samples were tested in-cell at Proton and showed much better operational properties than the uncrosslinked samples. Samples exhibited longer run times than previous non-cross-linked samples as well as improved stability. Prior uncrosslinked samples operated for less than 10hrs and had mechanically failed upon disassembly. The new cross-linked samples operated for 17hrs before the test was halted and were still intact upon disassembly. Testing results are shown in **Figure 25** below.

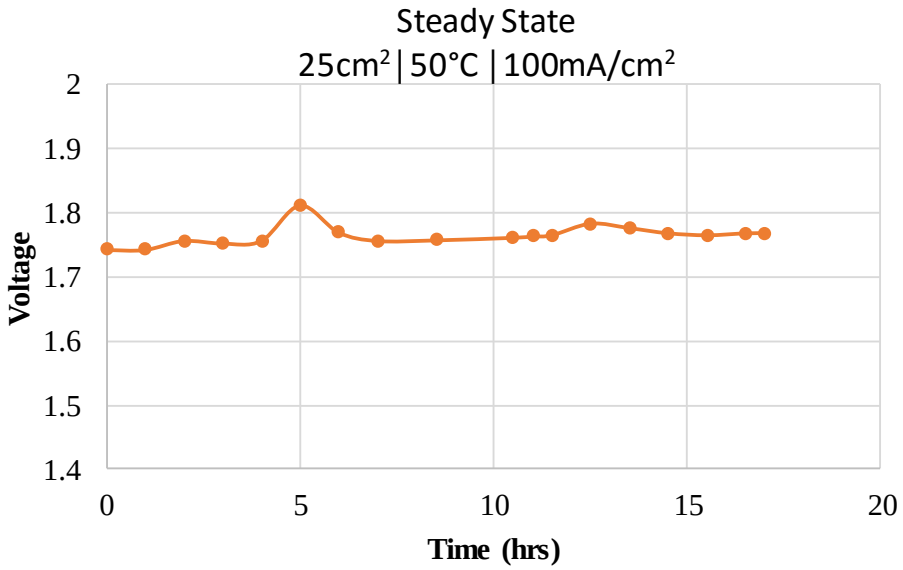

Figure 25: Steady-state operational data for crosslinked samples from PSU

Membrane stability

Degradation was measured in tested samples by comparing IR spectra before and after (**Figure 26**) in order to further improve stability. Generally, for operated samples, the CH_2 to CH_3 ratio decreased due to a decrease in CH_2 groups in the polymer. The decreased CH_2 to CH_3 ratio is consistent with both benzyl attack and Hoffman elimination although the exact degradation mechanism in an operating cell is unknown.

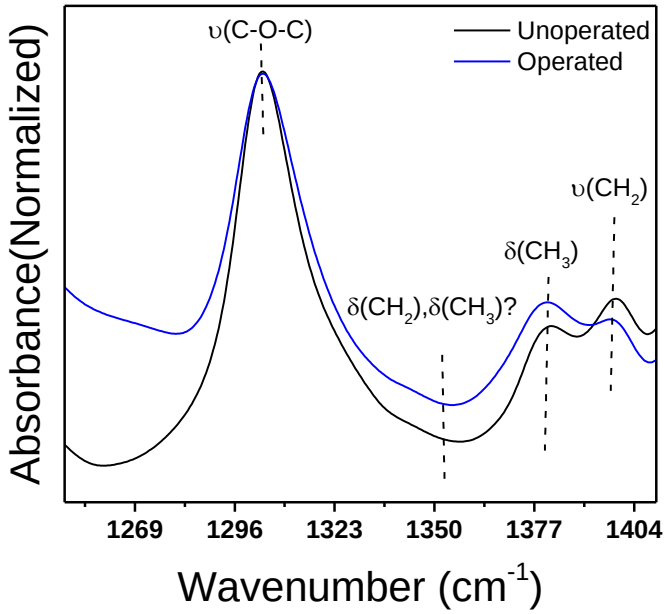

Figure 26: IR spectra of membranes before and after operation showing the change in the CH_2 and CH_3 bands.

A wide range of samples and conditions have been tested using this approach. The data is partially summarized in **Figure 27**. The figure shows that many conditions tested lead to some degradation as indicated by a CH_2/CH_3 ratio of less than 1 (dotted horizontal line). Although sample #7 appears

to have the least amount of degradation, it should be noted that cell operated for the least amount of time before failing mechanically, so it is likely that degradation was not observed due to the short duration of run time accumulated.

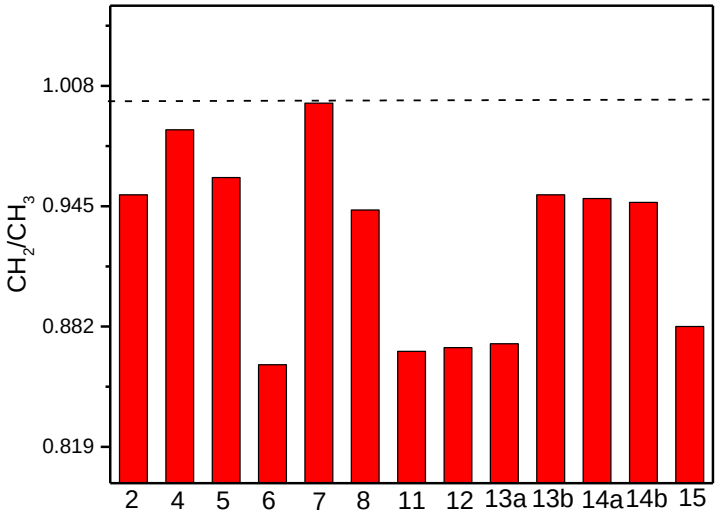

Figure 27: Partial list of samples and conditions for degradation experiments showing some degradation (CH_2/CH_3 ratio < 1) for many samples tested.

Final Membrane Durability Test

After the improved performance characteristics of the X27Y33 samples were verified by device testing, supported membranes were fabricated with a number of different porous inert supports. Mesh supports and designed supports from Dexmet corporation were used as substrates for fabricating supported AEMs with the X27Y33 ionomer. Photographs of the supported membranes are shown in **Figure 28**.

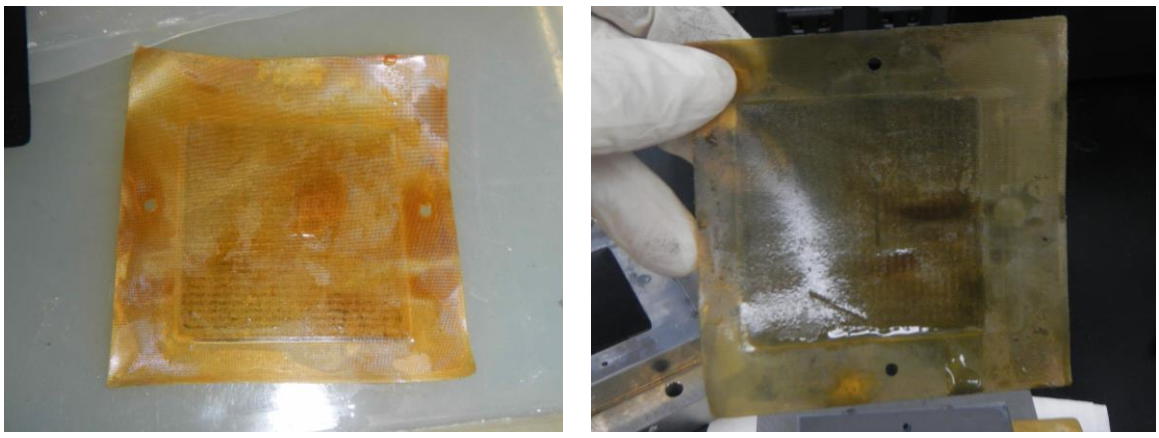

Figure 28: Photographic examples of mesh-supported AEMs

Supported membrane performance with the Dexmet materials proved promising; supports and chemically stable ionomers are the path forward to long-lived AEMs in electrolyzers. Final testing at Proton showed a significant improvement in performance with a 28cm^2 cell stack based on Proton's commercial hardware. Test conditions were 35°C and 200 mA/cm^2, with PGM catalysts being used in the OER and HER electrodes. In addition, differential hydrogen pressure was

maintained at 40 psi for the test duration. The results of the steady-state testing are shown below in **Figure 29.**

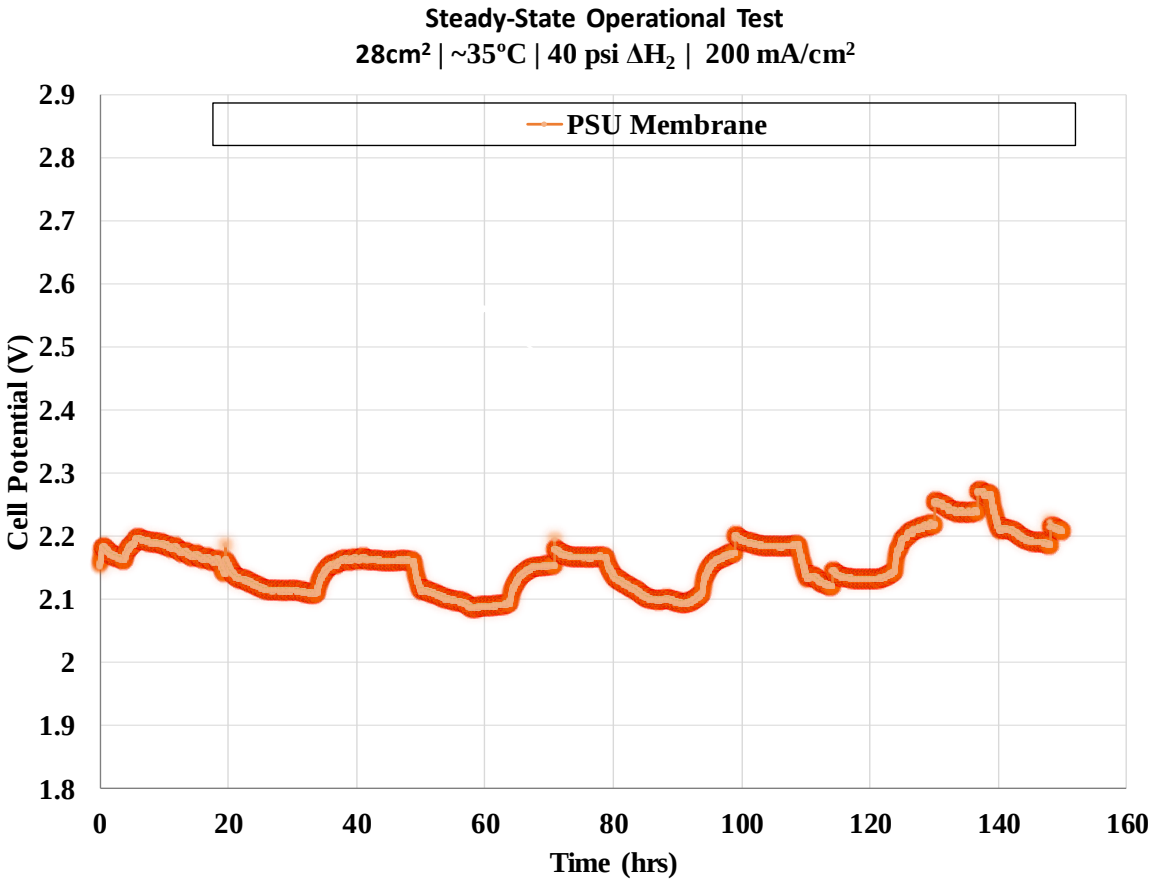

Figure 29: Steady-state operational data for reinforced PSU membrane

Conclusions

During the course of the project PSU was able to significantly improve the durability of their AEM. Leveraging feedback from Proton generated during the fabrication process and in-situ device testing, PSU iterated on compositions and configurations until improvement in operating time was demonstrated without evidence of failure. Further refinement was realized when Proton engaged a supply partner from previous projects to provide a mechanical reinforcement thin enough to be molded with the PSU ionomers. The additional of the reinforcement extended the operating time to 150 hours before the test was halted. Samples were returned to PSU for post-operational analysis to look for evidence of chemical degradation. This was still pending at the time of this report, but it is expected that PSU will continue to explore this membrane composition and reinforcements as a means to extend membrane operational life.

Task 3.0 Characterization of Catalyst Materials for HER &OER

Technical Approach

The interface between the support and catalyst layer can be visualized by cutting cross-sections using focused ion beam (FIB). SEM images can be then acquired to study the morphology of the catalyst layers itself and its interface with support. Digital Image Processing (DIP) of SEM images

allows for the extracting of parameters from images providing descriptive morphology for comparison purposes.

The objectives of in this task were to:

- Perform cross-sectional secondary electron imaging of electrodes using Focused Ion Beam
- Study differences in morphologies of electrodes made with different ionomer binder and top coat
- Follow the changes in morphology of electrodes as a result of operational testing pre and post operation – beginning of time (BOT) and end of time (EOT)

3D analysis of electrode structures (University of New Mexico)

The samples analyzed by UNM are listed in **Table 4**. Focused Ion Beam was used to create large (150 x 130 microns) cross-sections of electrodes. The platinum cap was deposited to protect the sample from the ion beam. Gallium ion source at the lowest current was used to cut the material to minimize sample damage. An FEG electron source at low voltage and low current is used to image the interface. High-resolution SEM images at 25X were then acquired from multiple areas within images **(Figure 30**).

Sample	Type	Catalyst	Support	Ionomer/ binder (in ink vehicle)	Top coat (applied on electrode surface)
1	PEM anode baseline	IrOx	OER GDL	Nafion	Nafion
2	AEM anode baseline	IrOx	OER GDL	Nafion	AS-4
3	AEM anode alternative	IrOx	OER GDL	AS-4	AS-4
4	AEM anode alternative tested	IrOx	OER GDL	AS-4	AS-4
5	BOT 1	IrOx	OER GDL	AS-4	AS-4
6	BOT2	IrOx	OER GDL	Nafion	AS-4
7	EOT 1	IrOx	OER GDL	AS-4	AS-4
8	EOT2	IrOx	OER GDL	Nafion	AS-4

Table 4: University of New Mexico successfully analyzed eight electrode structures

Figure 31 shows high-resolution images for electrodes test samples 1-3 illustrating different types of structures observed. GDE 1 and 2 have similar areas of uniform morphology and some areas with larger pores, as shown in the GDE2 bottom images. GDE 3 has areas of very compact morphology with small pores and non-uniform morphologies.

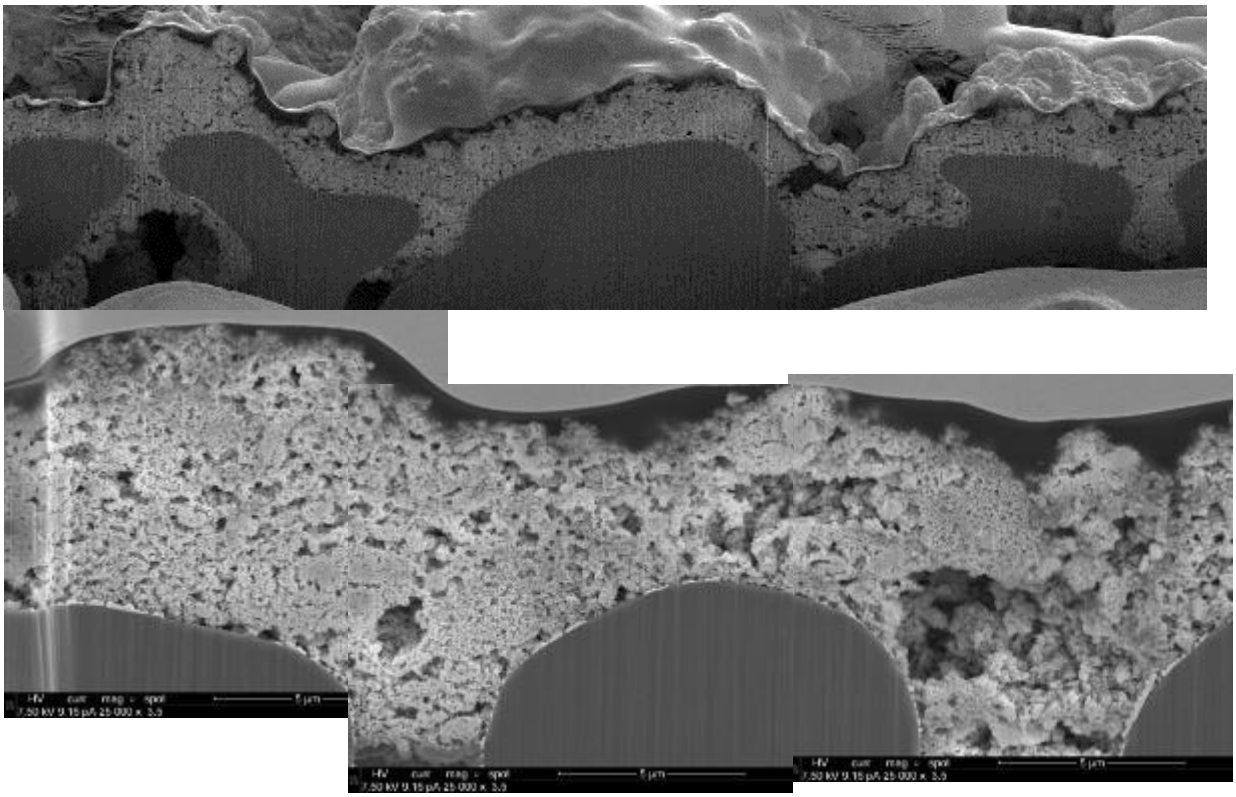

Figure 10. Top - large cross-sections with an overall view of electrode and support. Bottom - high-resolution SEM images

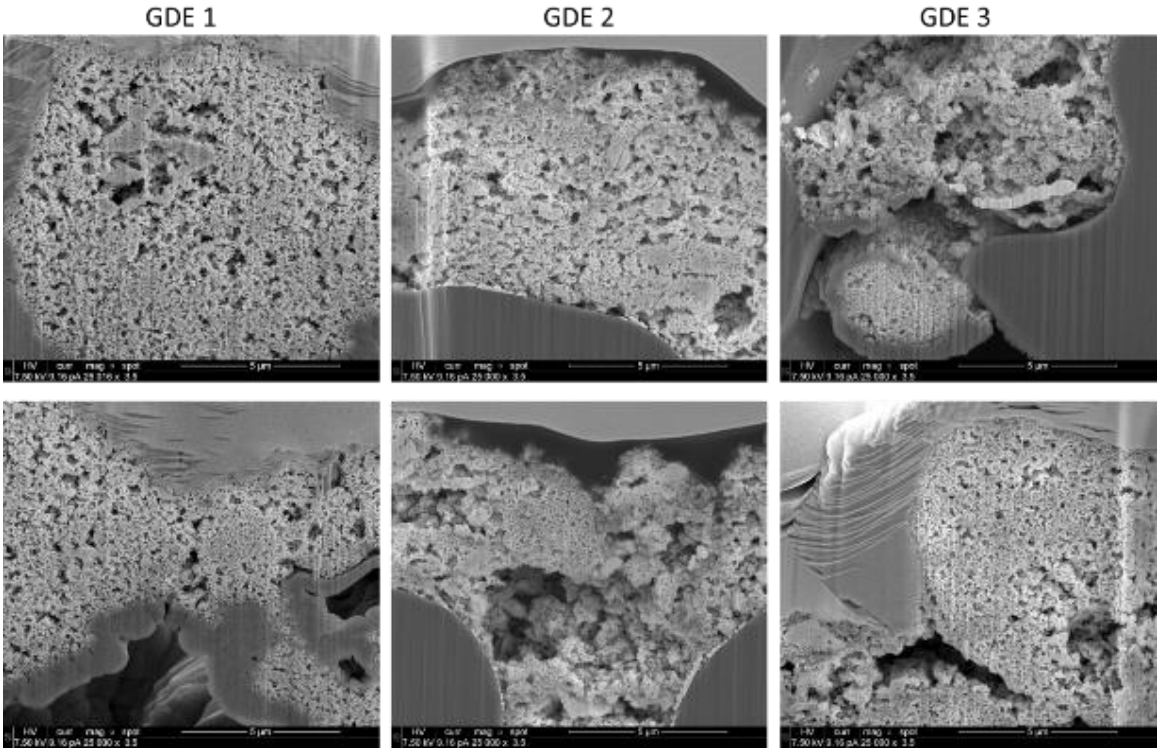

Figure 31. High-resolution SEM images from 1-3 electrodes

Figure 32 shows a large cross-section and high-resolution images of the BOT #3 and EOT electrode #4. The very heterogeneous structure of both fresh and tested electrodes does not allow derivation of any conclusions on changes occurring during the test. Only through the application of digital image processing described below, it was possible to analyze the changes in morphology.

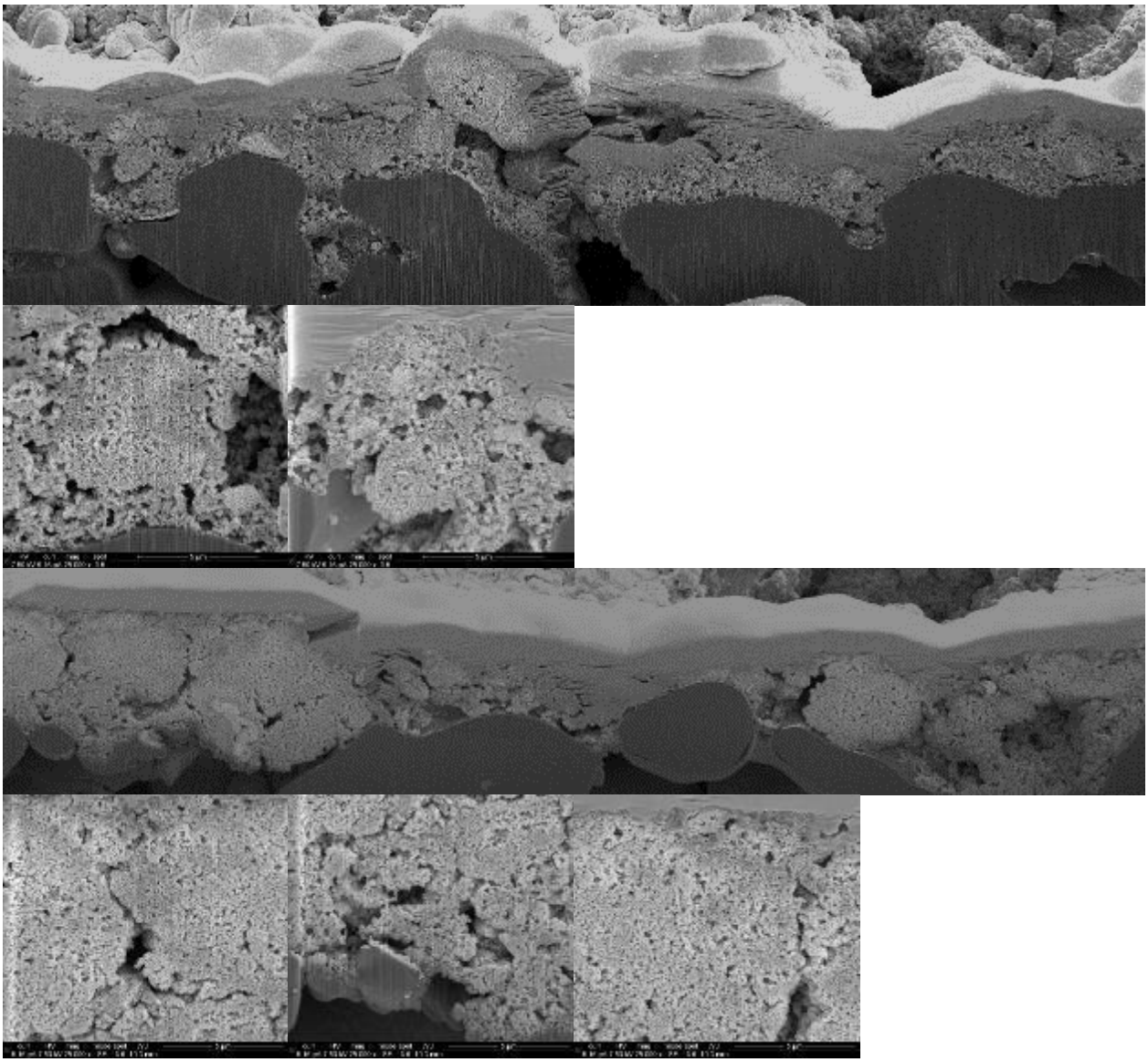

Figure 32. Cross-section and high-resolution SEM images from electrodes 3 (top) and 4 (bottom)

Figure 33 shows large cross-section and high-resolution images for two fresh electrodes 5 and 6 and the same electrodes after the test (electrodes 7 and 8, respectively). In electrode 7 after the test, there is a loss of the porosity observed vs electrode 5 before operation. For electrode 6, the opposite was observed after test – with more pores visible in electrode 8 than in electrode 6.

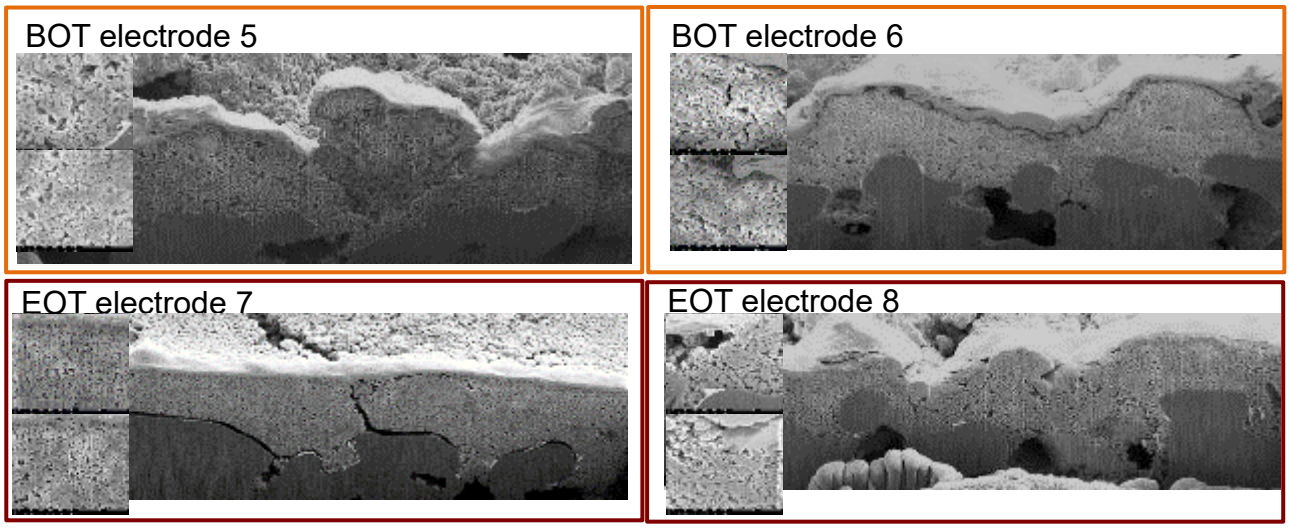

Figure 33: Large cross-sections and high-resolution SEM images from electrodes 4-7

Digital image processing

To quantify the electrode morphology, digital image processing (DIP) was performed. A set of 6 x 6-micron areas were cropped from each image to focus specifically on catalyst layers. (see **Figure 34**)

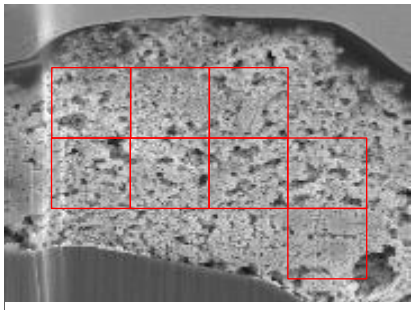

Figure 34: Cropping images for DIP

For the images collected, roughness, textural, and areal parameters were calculated:

A. Roughness represents overall heterogeneity of material
B. Skewness – measures the amount of pores (the smaller the number, the more pores present)
C. EP – measure of connectivity – the more negative, the better connectivity in pores
D. Fraction of solid in % is inverse of overall porosity
E. Average solid phase size in horizontal (X) and vertical (Y) direction in pixels (1 pixel =15 microns)
F. Average pore size in horizontal (X) and vertical (Y) direction in pixels (1 pixel =15 microns)

The average, maximum, and minimum of all these parameters are presented to show the range in morphological properties, which are related to heterogeneity of electrodes. **Figure 35** shows results for three non-operated electrodes, samples 1-3. Electrode 1 has the most homogeneous morphology from area to area. The spread in morphological parameters is largest for Electrode 3. Electrode 1 is the least rough with smaller pores. Electrodes 2 and 3 have a large range of porosities, captured by skewness, indicating heterogeneity with some areas having many pores or large pores and other being denser or having much smaller pores. The fraction of solids is lower for electrode 1, which has more pores present than in electrode 2 and 3. Average dimensions of the solid phase are very uniform and smaller for electrodes 1 and 2. Sample 3 has a large spread in size of solid phase reaching up to 300 nm. The average size of pores is smallest for electrode 1, while electrodes 2 and 3 have a larger range of pore sizes. Overall electrode 3 is much more heterogeneous than the other 2 electrodes. A large spread of morphological properties are detected with some areas being very compact with small pores, and some areas having very large holes detached from Ti support.

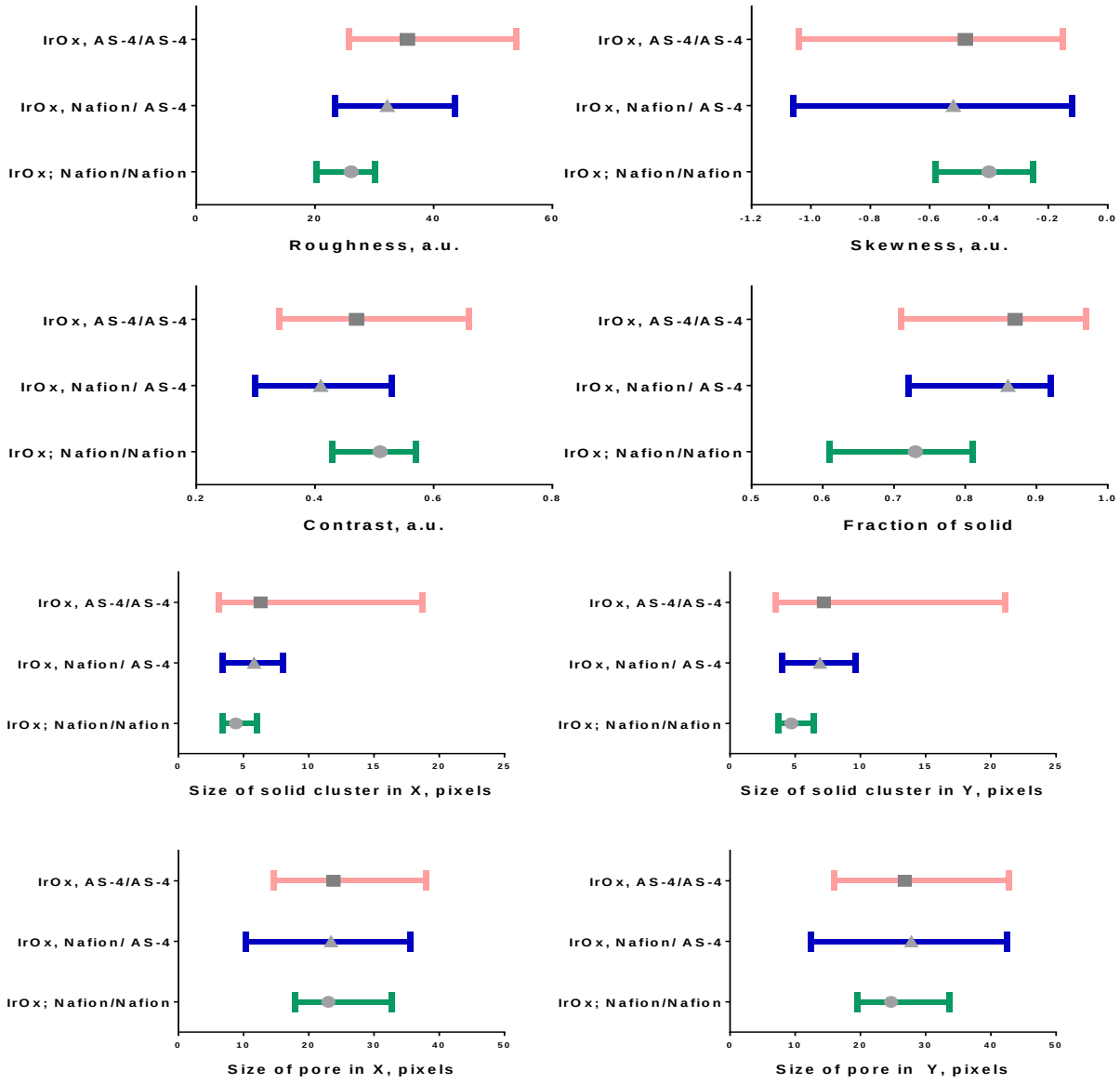

Figure 35: Morphological parameters for electrode 1-3

Figure 36 plots morphological parameters for non-operated sample 3 and after test sample 4 GDEs. Roughness is almost unchanged after the test. A larger range of skewness is observed after test, pointing towards the formation of areas with a larger number of pores. Increase in EP due to loss of connectivity in pores is observed in the tested electrode. The observed decrease in solid fraction would also be attributed to porosity growth. An in increase in the size of the solid phase and a decrease in the pore size would indicate the collapse of the electrode structure.

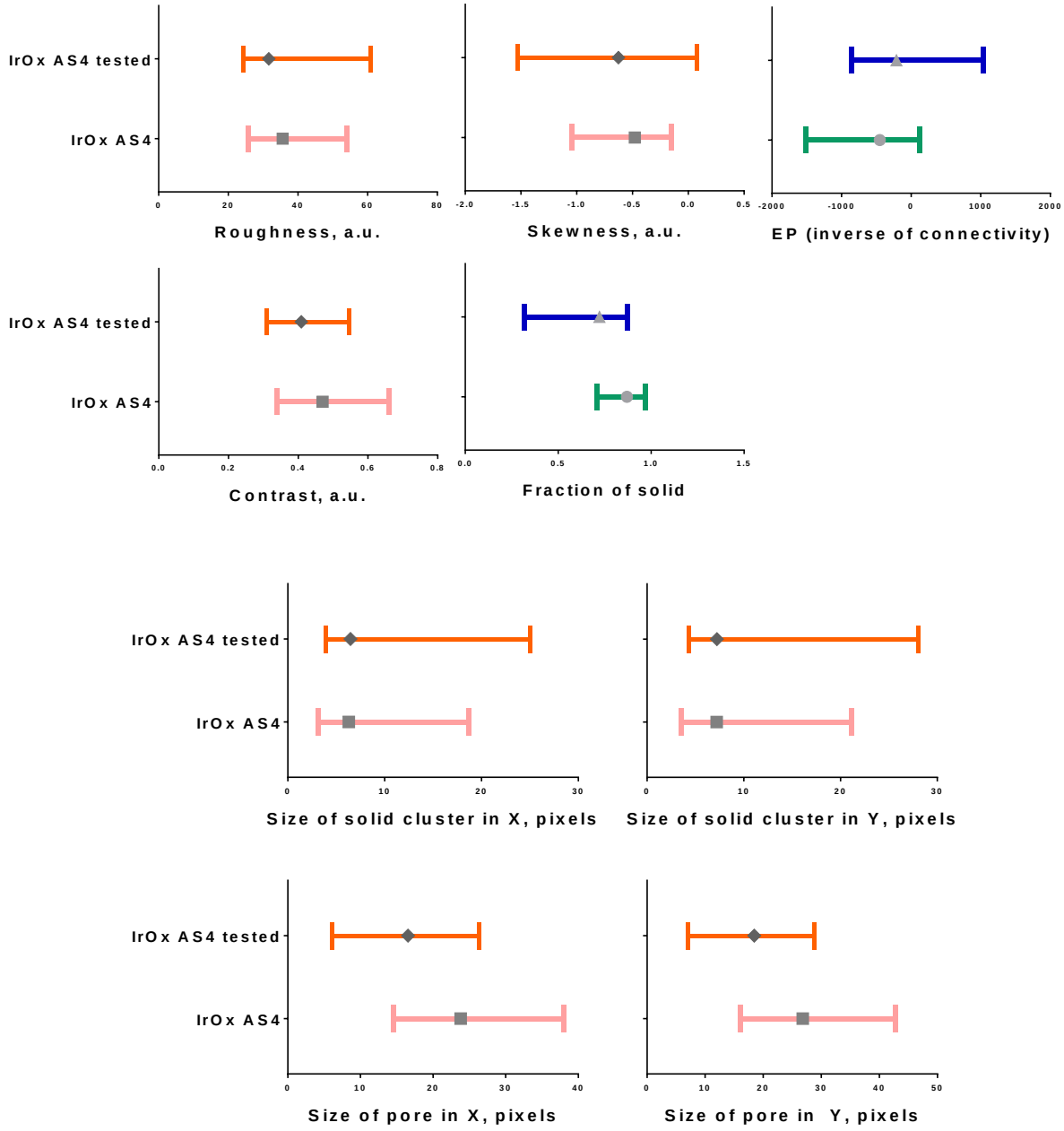

Figure 36: Morphological parameters for electrodes 3 and 4

Figure 37 shows the comparison between non-operated and operated electrodes of two different binder configurations, based on AEM and PEM ionomers (electrodes 5 through 8 shown). Very different changes are observed after test of AS-4 and Nafion-based electrodes. The roughness of the AS-4 electrode decreased with smaller pore sizes and smaller solid phase size after the test. Loss of porosity is also observed due to the collapse of the electrode. For the Nafion–based electrode, the porosity and roughness increased after the test, accompanied by the growth of pore size and solid phase size. Thinning of AS-4 and expanding of Nafion-based electrodes was also observed after the operational test. It is believed that the Nafion increase in porosity helps to

improve transport and conductivity, while the collapse of the AS-4 electrode and loss of porosity has the opposite effect, reducing electrode performance.

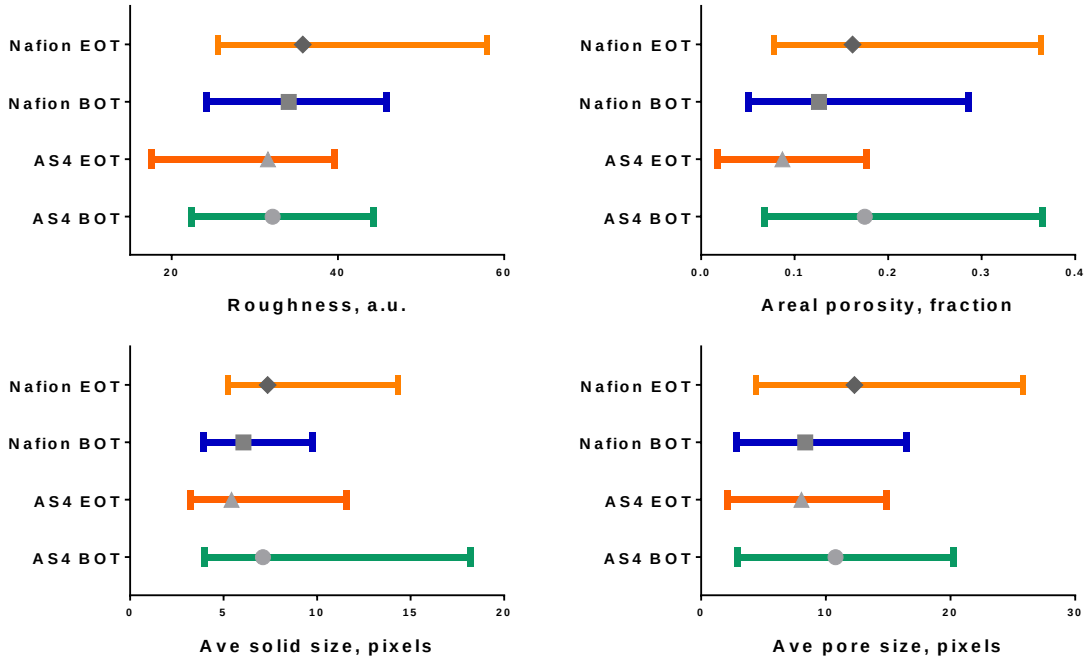

Figure 37: Morphological parameters for electrode samples 5,6,7 and 8

Task 4.0 Electrode Fabrication and Characterization of Interfacial Effects

Interfacial Effects

To understand the role of carbonate in contact with A201 membrane, NUCRET supported fundamental work to clarify the understanding of how this addition improves performance and stability. The following provides an update on microelectrode data, RDE, and liquid cell-observed half reactions.

Method

1. A Pt microelectrode was tested in 1% carbonate and 0.335% KOH (same conductivity-mS, but different pH).
2. RDE testing of drop cast PGM and non-PGM catalysts in 1% carbonate and 0.335% KOH was performed to study intrinsic HER and OER activity.
3. A liquid cell with a reference electrode in the liquid chamber was tested to study half reactions of HER (functioning as a hydrogen pump).
4. Interfacial effects: Microelectrodes in contact with A201 membrane were operated, when pure DI water is supplied vs. 1% carbonate vs. 0.335% KOH.

Results

Figure 38 shows the CV-Pt surface characterization on the left, while HER activity and how carbonate inhibits Pt performance is shown in the graphic on the right. Inhibition of the H-upd region appeared in carbonate electrolyte and thus, HER performance was much lower compared

to hydroxide electrolyte. NUCRET used a microelectrode having a flat Pt surface, as opposed to the uneven catalyst layer that results when drop-casting onto a RDE.

RDE results are shown in **Figure 39** for PGM and non-PGM catalyst in 1% carbonate and 0.335% hydroxide at 50ºC, mimicking the water splitting cell operating condition. In the case of OER, there were no significant differences in performance for the carbonate vs. hydroxide scenarios when PGM and non-PGM catalysts were compared. For the HER catalyst, NiCr/C, the change in performance was not as dramatic as the change observed in the Pt performance in the presence of carbonate. When these results are combined with the microelectrode data, it is believed carbonate has a negative effect on Pt, but the non-PGM NiCr/C does not appear to have this sensitivity.

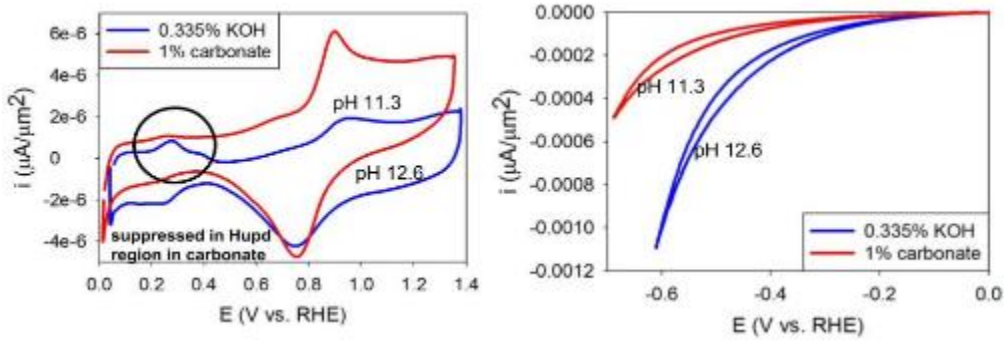

Figure 38: CV surface characterization (left) HER activity for Pt performance (right)

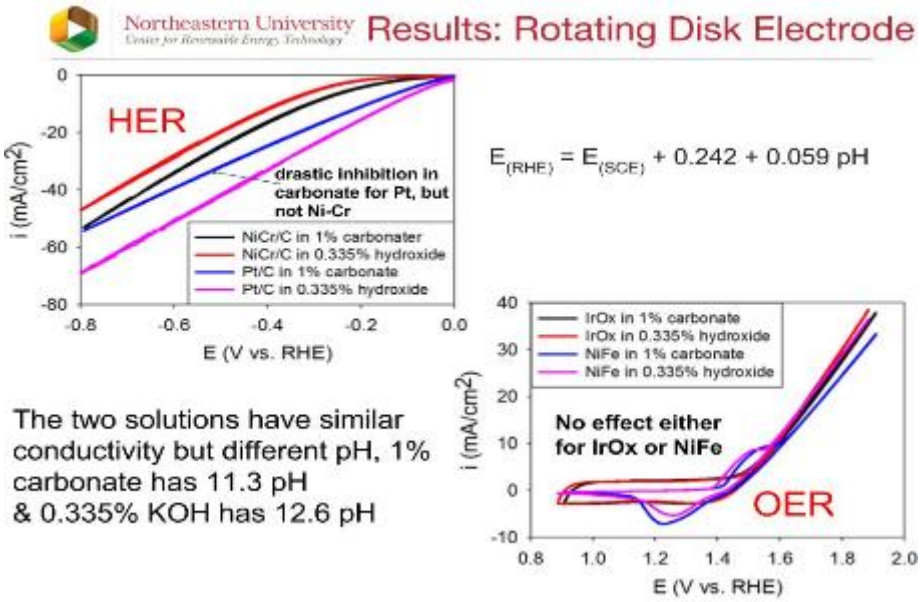

Figure 39: RDE results for HER (left) and OER (right)

Liquid cell:

A novel alkaline liquid electrochemical cell was used at NUCRET to evaluate performance as a function of solution (**Figure 40**). Two housing blocks, two graphite flow fields, two electrodes, a reference electrode, and a reference electrode housing comprise the liquid cell. The housing blocks and flow fields are mirror image assemblies. Hydrogen gas enters one housing block and flow field, while an alkaline solution, either potassium hydroxide or potassium carbonate, is supplied

to the opposite block and flow field. The liquid side electrode has a NiCr/C coated carbon cloth as the electrode, allowing passage of the alkaline liquid into the reference electrode housing. The gas side electrode is Teflon-coated carbon paper and Advent platinum on carbon catalyst, which blocks the passage of the alkaline solution into the hydrogen flow field while still allowing the passage of hydrogen gas into the reference electrode housing.

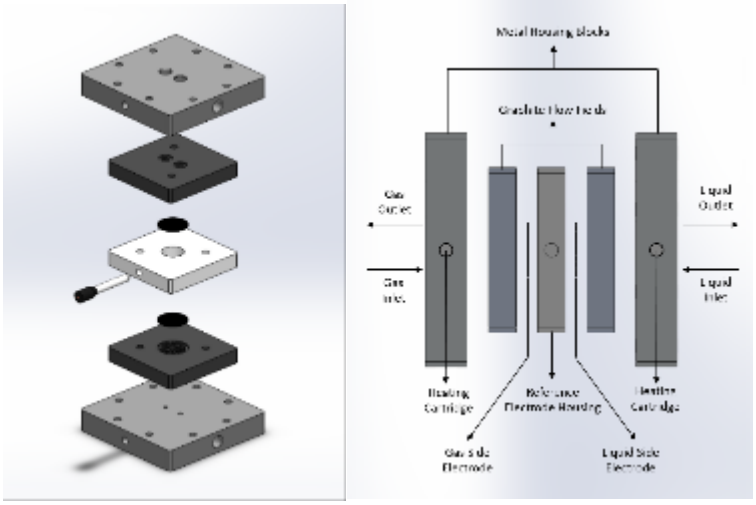

Figure 40: An expanded view (left) and diagram (right) of the novel alkaline liquid electrolyzer cell

Results

Two high concentration/conductivity solutions were used to compensate for the high resistance resulting from the large gap between electrodes in the electrolyte chamber. The SCE was used as the reference for pH dependence tests. **Figure 41A** shows the HER performance of NiCr/C in carbonate vs. hydroxide. **Figure 41C and 41D** show NiCr/C versus Pt/C in both carbonate and hydroxide solutions show the difference in half reactions for HER. Unfortunately, there was significant variability in conductivity for these high concentration solutions. A conductivity difference of 35 mS across the hydroxide to carbonate tests was measured in the NiCr/C experiment. Furthermore, the experimental setup did not have stable temperature control, the NiCr/C experiment hydroxide reservoir temperature was higher than the carbonate. The conductivity and temperature differences are both factors that would inherently impact performance. These differences have to be noted; however, a trend was observed in the case of Pt/C, where higher V vs. RHE (overpotential) was observed in the carbonate solution, even though the conductivity of the carbonate solution was higher than the hydroxide. This data works to further support the RDE and microelectrode data.

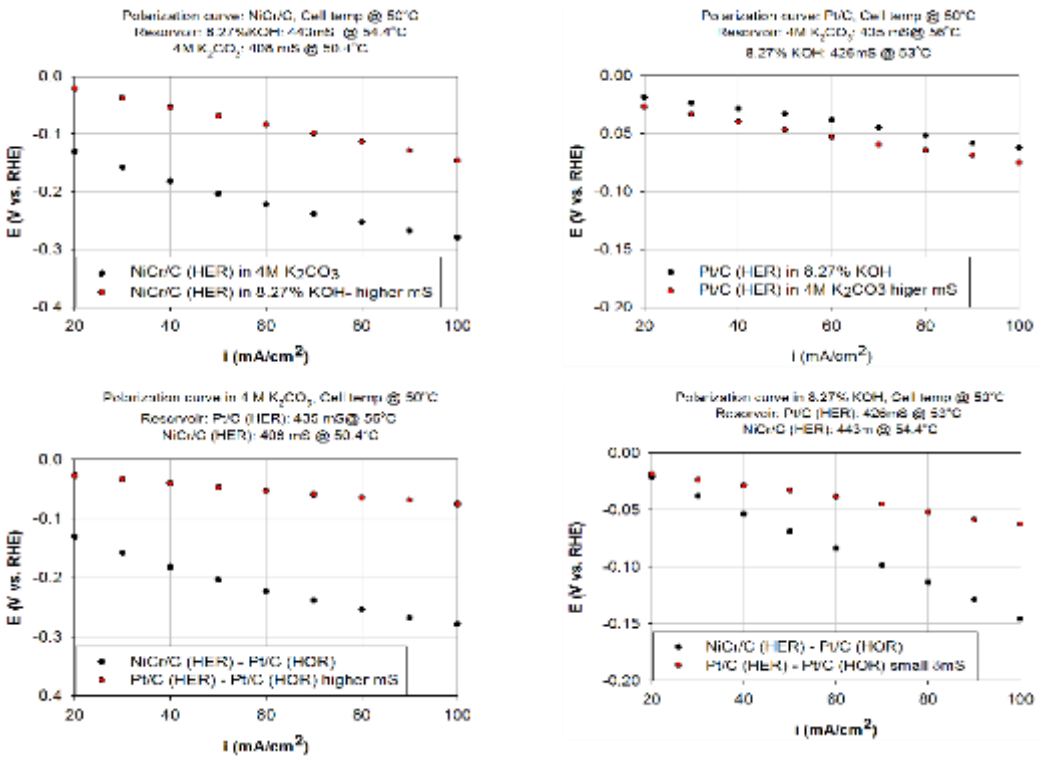

Figure 41: Polarization curve of NiCr/C **(A)** and Pt/C **(B)** in carbonate vs. hydroxide solutions NiCr/C **(C)** vs. Pt/C **(D)** in carbonate and hydroxide solutions

Electrode Fabrication

Throughout the program, Proton On-Site was able to successfully incorporate non-PGM catalysts for the hydrogen evolution reaction (HER) and oxygen evolution reaction (OER) into single cell bench tests for electrolysis screening. Using these non-PGM catalysts provided by NUCRET and feeding the cell with 1% carbonate solution, all operational milestones were achieved.

Test and Down-select (Proton)

Non-PGM catalysts provided by NEU were successfully incorporated into electrodes. Materials were selected based on previous results for the OER final down-selection, as well as recent findings in performance and stability for the HER materials. NiFe/Raney and NiFeCo were tested in a 25cm^2 cell to look for stability and performance. Testing was conducted with 1% carbonate feed to the anode at 50ºC. The steady-state results can be seen in **Figure 42** below, with the NiFe/Raney showing stability and higher performance at 500 mA/cm^2 versus the NiFeCo, which was unstable and less efficient, even though the current density was limited to 200 mA/cm^2. NiFe/Raney was selected as the OER catalyst for the final program durability milestone.

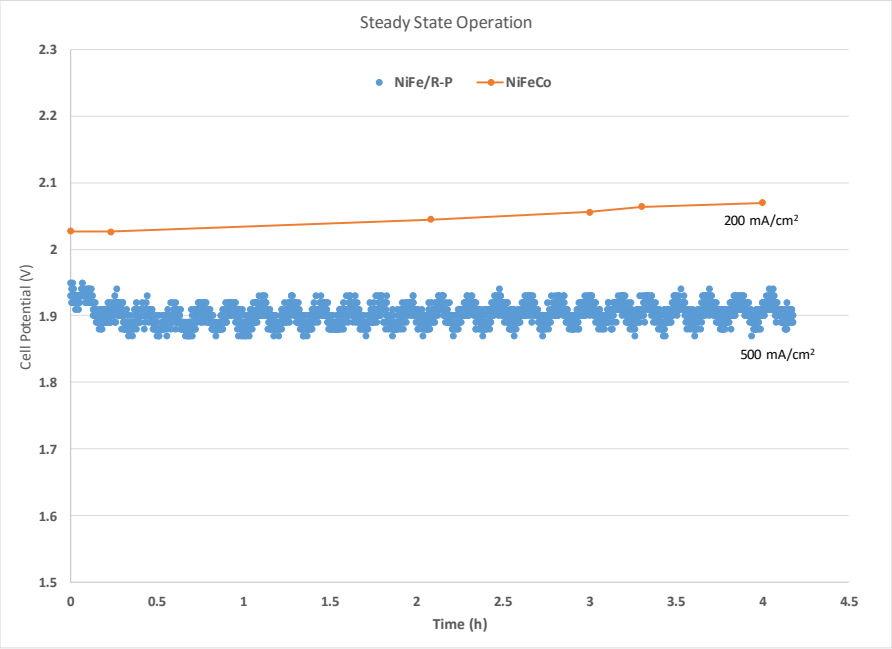

Figure 42: Steady-state operational testing for OER down-selection collected at 50ºC

NiCr/C, NiCr, and NiNx/C were incorporated into electrodes and tested as HER candidates. Steady-state operational data was collected using counter electrodes made from traditional PGM catalysts to isolate the performance of the HER electrode. All testing was conducted with carbonate supplied to the anode side of the cell at 50ºC. As shown in **Figure 43**, the NiCr/C and the NiCr samples could not achieve the target current density of 500 mA/cm^2 with NiCr/C showing instability at 400 mA/cm^2 and NiCr showing some stability, but only at 100 mA/cm^2. NiNx/C was therefore chosen as the HER catalyst for the final durability milestone.

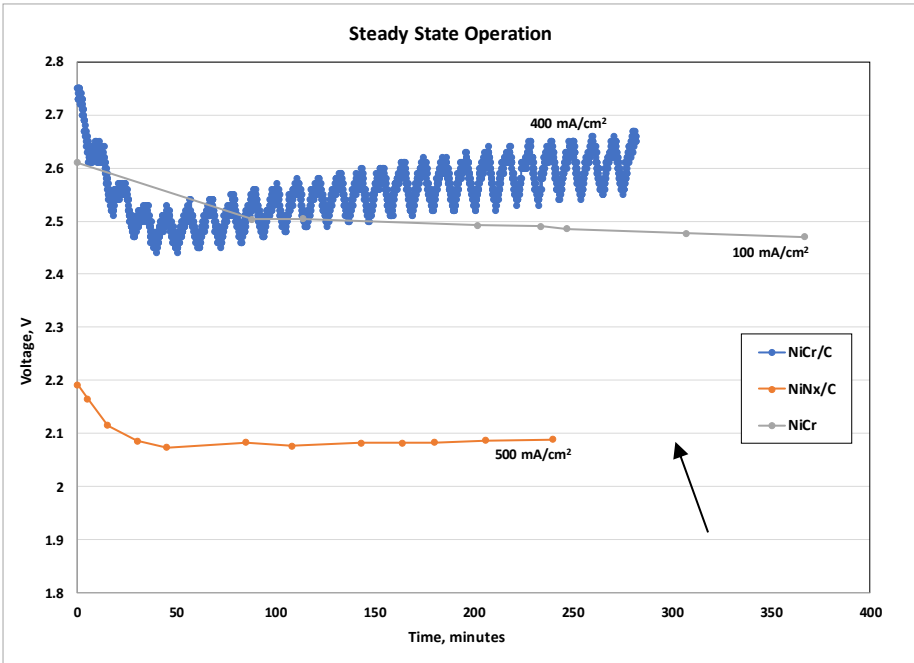

Figure 43. Steady-state operational testing for HER down-selection collected at 50ºC

Full non-PGM Testing

Building on the previous successes with discrete HER and OER electrodes, full in-cell testing was conducted. GDEs were processed using the previously tested catalysts provided by Northeastern University and a full in-cell test was planned at Proton with non-PGM anode and cathode using Tokuyama's A201 membrane. This test was the first to operate using a full non-PGM water electrolysis cell configuration. Operational testing was conducted in the 25 cm^2 hardware, with the addition of carbonate to the feed water and parameters set to 80ºC and 500 mA/cm^2. The target for the **year 1 milestone (Q4)** was to achieve a 2.0V cell potential for full non-PGM operation. **Figure 44** below shows a relatively flat voltage trend at the target potential, indicating no loss of catalytic activity over the test, successfully meeting the quarterly milestone target.

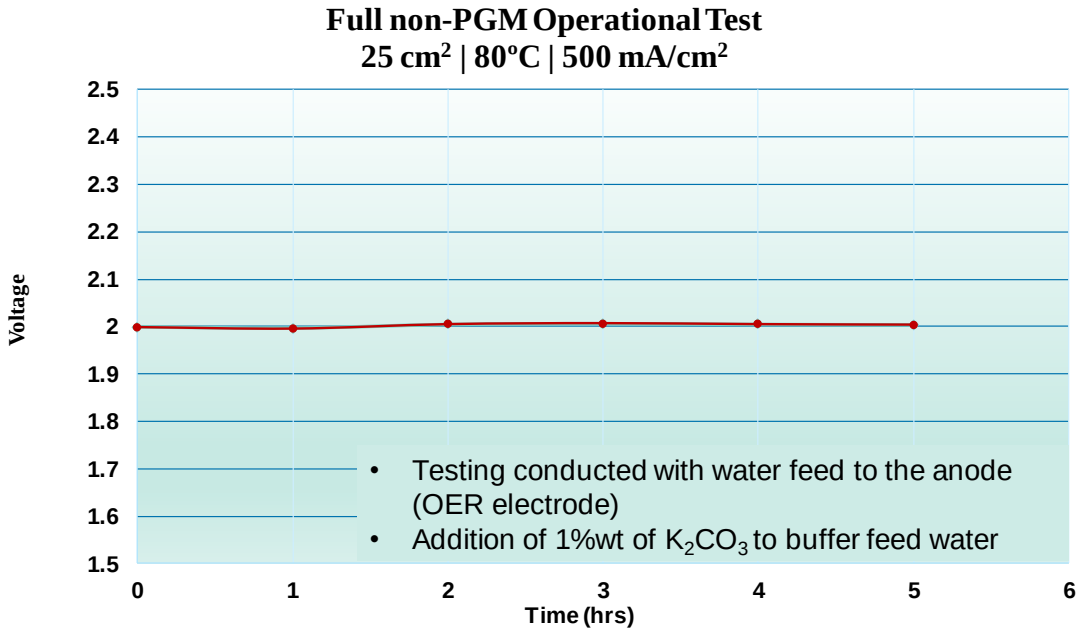

Figure 44: Operational testing of a full non-PGM anode and cathode GDE in an AEMWE cell. Feed water temperature of 80 ºC and buffered with bicarbonate

Electrodes were then integrated with Proton's 28 cm^2 commercial cell hardware for longer term operational testing, with the addition of carbonate to the anode feed water and parameters set to 35ºC and 200 mA/cm^2. As shown in **Figure 45** below, the non-PGM cell successfully showed relative stability over the course of its 200-hr test. This result indicates a robust electrode that remained intact throughout the test duration, and set a new steady-state bench-mark for accumulated hours on a non-PGM cell. The stack was eventually removed due a failed pump on the system and would have been allowed to continue if this fault hadn't forced the shutdown.

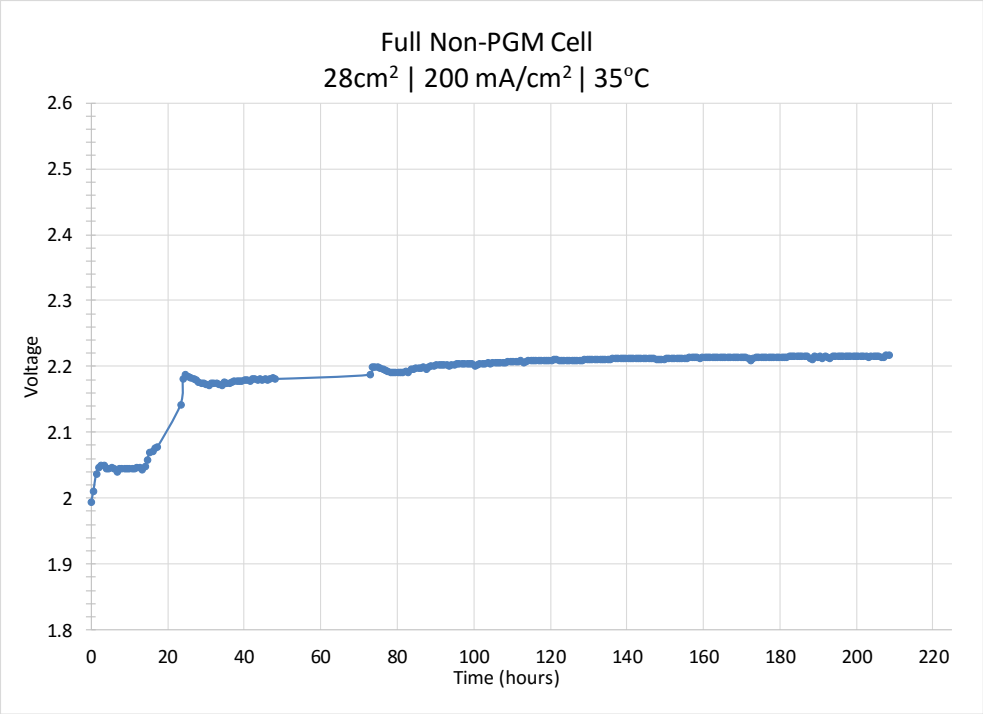

Figure 44: Operational testing of a full non-PGM anode and cathode GDE in an AEMWE cell. Feed water buffered with carbonate

Task 5.0 Cell Engineering

Background

Under this program, a fixture was designed to provide a way to visually see the water transport through a membrane (**Figure 45**).

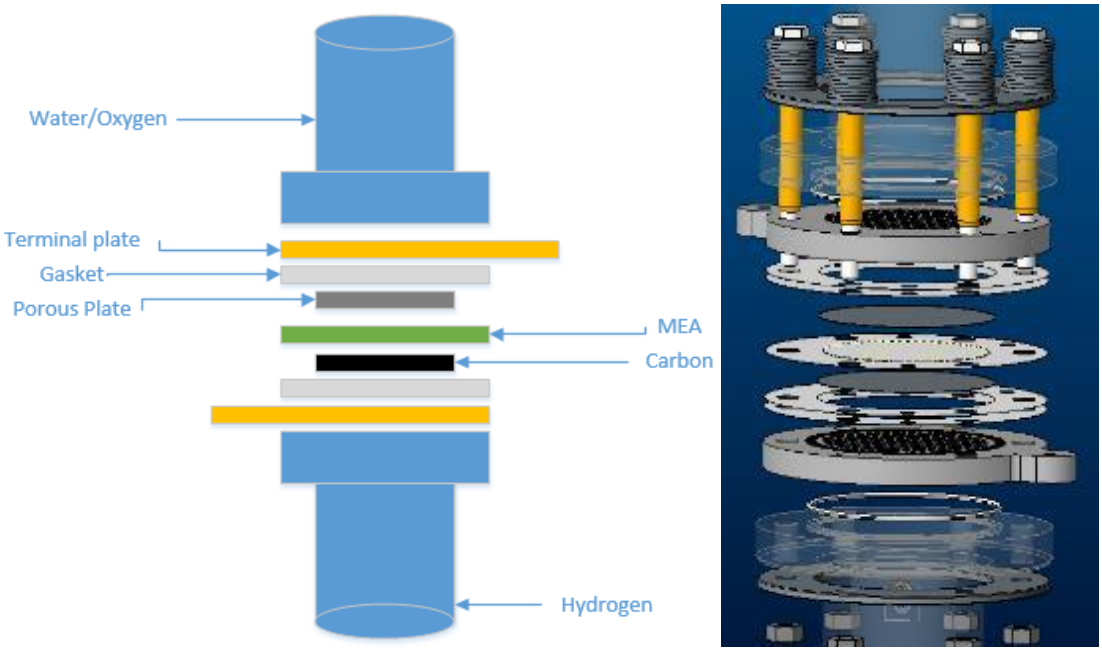

Figure 45: Layers of Water Transport Fixture

The intent was to be able to measure the water flux through a given membrane under differential pressure with a current applied. The clear design allows for real-time visualization of the water interaction on the anode, as well as the influence of hydrogen differential pressure and GDL configuration on water management for both sides of the cell. To simplify the design and reduce the number of unique parts, the GC cell stack was leveraged as the starting platform of this water transport fixture. The maximum allowable working pressure for this system is 200 psi at up to 28°C. This pressure/temperature range is adequate for testing, while still providing a safe working environment.

Design

The upper and lower vessels allow for a volume of 75 mL each of DI water to be filled or collected. This component had to be made from a clear plastic to allow for the visual aspect of this design. Polycarbonate was the material of choice, and many calculations were done to ensure that the endplate would be safe at the design pressure of 200 psi. An FEA analysis was also completed, and results were compared to the hand calculations.

Figure 45 and 46 show the results of the FEA modeling and high stress areas in the vessel. The points of concern were at the fitting port and at the area of bolt clamping. Both areas showed a high enough safety factor to feel confident in the design at a proof pressure of 300 psi.

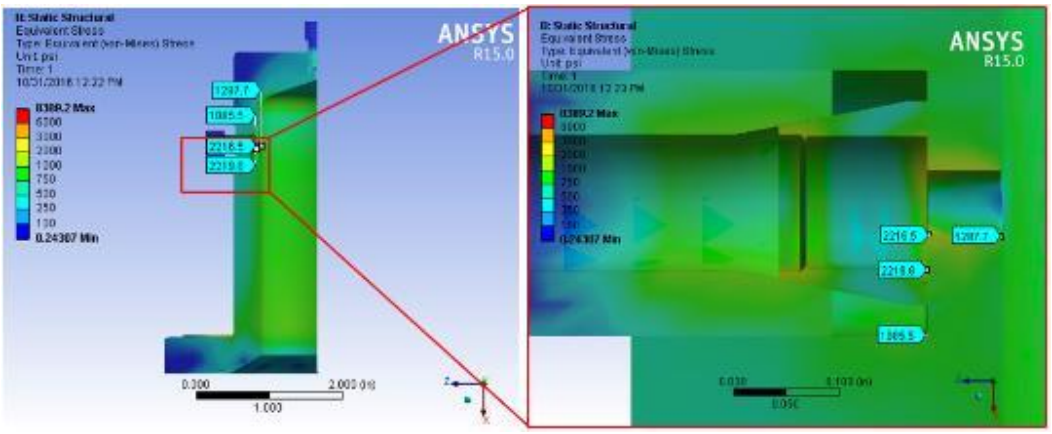

Figure 45: FEA results for endplate – Stresses at port

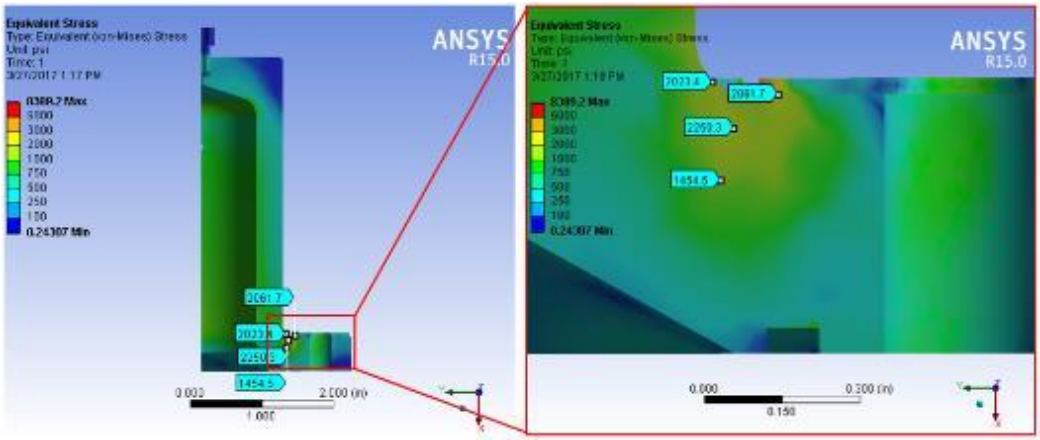

Figure 46: FEA results for endplate – Stresses at washer to endplate interface

An FEA analysis was also completed for the terminal plate (**Figure 47**). This analysis was done to determine the thickness needed to ensure the component deflection would be below 0.001".

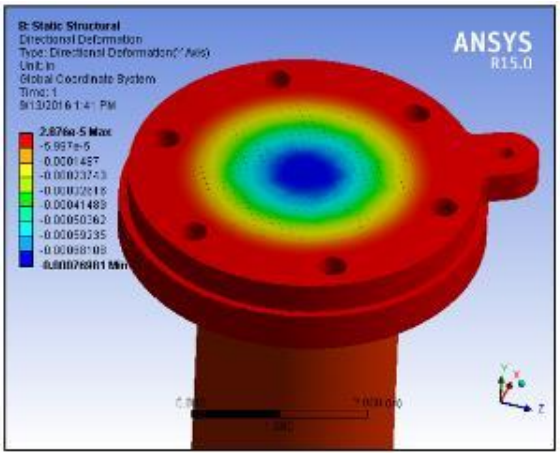

Figure 47: Max deflection of 0.0008" on terminal plate, below target of 0.001"

The endplate is ported to allow for the filling and collection of water. The fittings chosen for this application are from IDEX; a PEEK nut and an ETFE ferrule combination. These fittings are rated for up to 500 psi. This pressure rating allowed for both the port and fittings to be plastic.

The terminal plate is assembled in between the endplate and the cell assembly. The endplate to terminal plate interface is sealed using an O-ring (The terminal plate to cell assembly (Seal gasket) interface is sealed using ridges on the terminal plate. For water to pass through the membrane to the cathode side of the cell assembly, it must flow through the terminal plate. Many holes were machined into the 3/8" thick terminal plate to allow for this water flow. The fully fabricated vessel is shown in **Figure 48**.

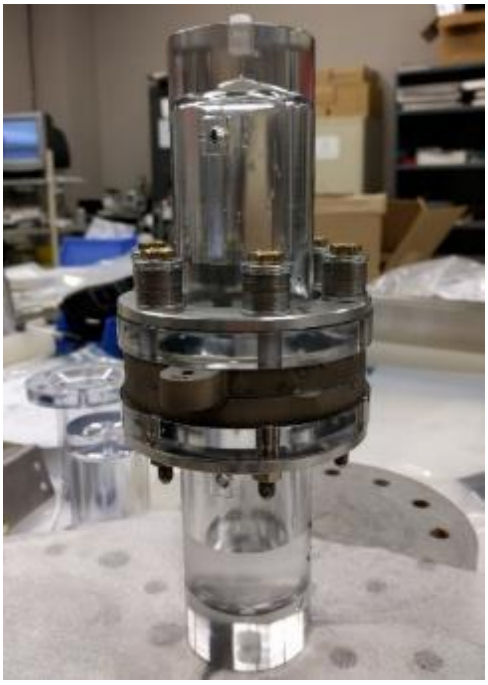

Figure 48: Full assembly of Water Transport Fixture

To ensure there is protection to all operators, the water transport fixture operates inside an enclosure in case there is ever an overpressure incident involving a mixture of H_2 and O_2. The enclosure (**Figure 49**) is made from Lexan so the visual aspect of the test stand is still maintained. Calculations were completed to determine the thickness of this enclosure and these calculations, based on past projects, indicated that ½" thick would be adequate to use.

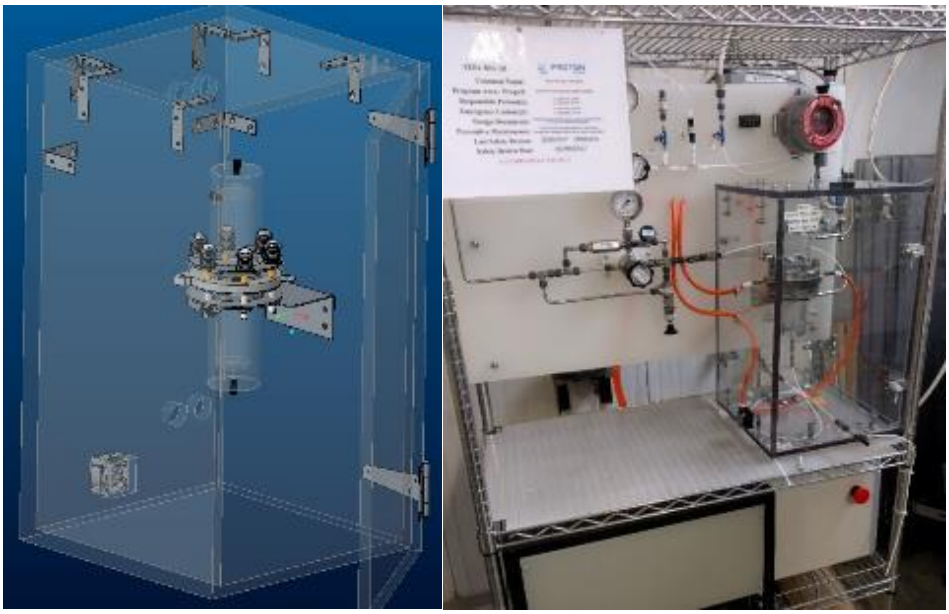

Figure 49: Designed enclosure (Left); Final test stand (Right)

Once the design and analysis of all components was completed and prototype parts received, a hydrostatic test was completed on the full fixture (**Figure 50**). The goal of this test was to achieve proof pressure with no leaks, cracks, or crazing observed. The test was successful at the proof pressure of 300 psi, showing only a 3 psi drop over 5 minutes, which is well below the Proton standard allowable pressure loss of 5 psi/min.

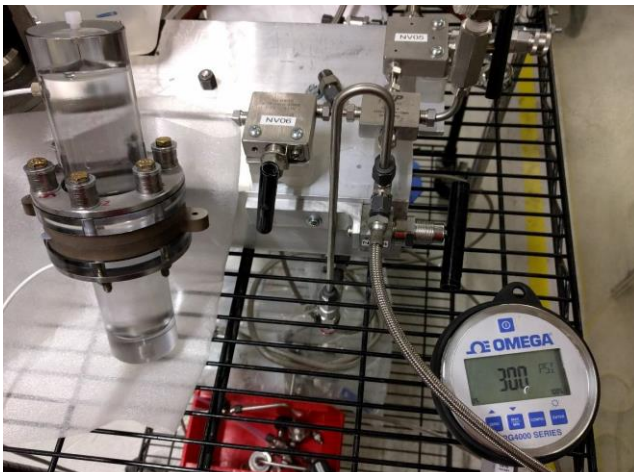

Figure 50: Hydrostatic test performed on 2/16/17

Going forward, the water transport fixture will be a valuable way to test different membrane materials under various operating temperatures and pressures to characterize the water flux

through the membrane. This will help classify membranes and determine how each performs in different situations.

Task 6.0 Prototype/System Demonstration

The development of a dual feed AEM test stand was completed to add testing throughput and test stand functionality for different operating modes. System safety review and documentation release was conducted prior to operation and was functionally verified before full test scenarios were introduced. Testing was specific to 25 cm^2 AEM operation. **Figure 51** below shows the fully fabricated system resulting from this effort. In addition to the expectation that K_2CO_3-doping would improve cell performance, it was expected that operating a cell with water fed to the cathode, doped or not, would improve performance because the cathode is where the water splitting reaction takes place.

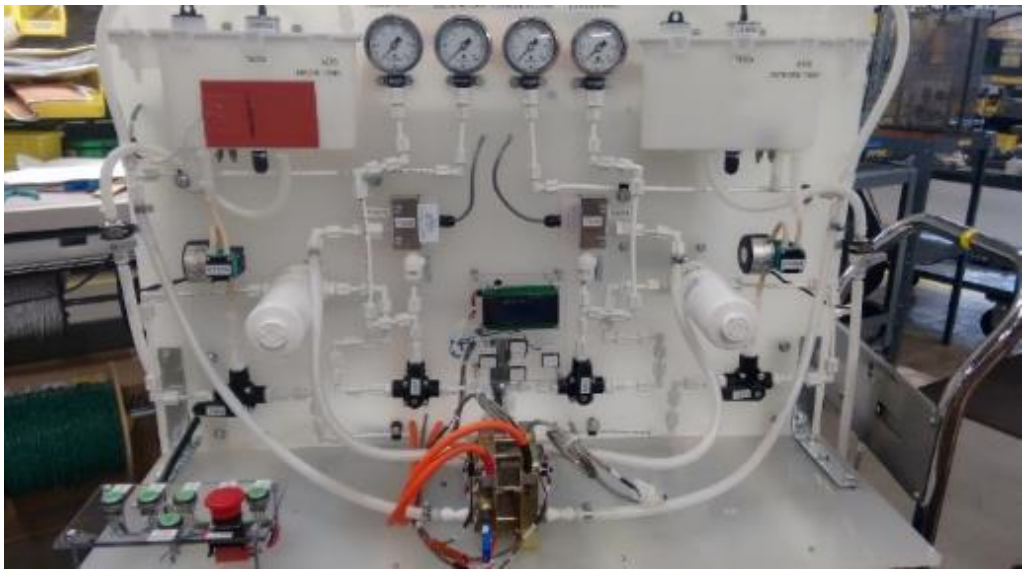

Figure 51: full system post assembly

An important feature of the membrane electrolysis approach to hydrogen generation is its ability to generate pressurized gas without a mechanical compressor, which requires a much more complicated balance-of-plant design when the product gas and the water return streams are the same. PEM systems feed to the anode side of the cell and produce product hydrogen on the cathode side of the cell, so the product chamber can be kept at the delivery pressure and the water feed can remain pressurized only by the pump. This test plan was developed to quantify the differences between operating a cell with an inlet water flow to the anode, cathode, or both in order to define the requirements of an AEM hydrogen generation system. In addition to the inlet flow position, the study looks at the effects of doping the water feed stream with a potassium carbonate (K_2CO_3) buffer and using a hydrophobic anode GDL in the cell. It was expected that K_2CO_3-doping would improve cell performance and the ability to provide water fed to the cathode, doped or not, would improve performance because the cathode is where the water splitting reaction takes place.

Methods

Dual feed testing was conducted in a 25 cm^2 test cell at ambient operating pressure. The cell was integrated into a specially-made test stand designed to readily allow switching flow on and off between the anode and the cathode sides of the cell. This stand is pictured in **Figure 52**.

All testing was conducted at 50°C with A201 membrane and gas diffusion electrodes (GDEs) as the anode and the cathode, comprised of PGM catalysts. Prior to building up the cell, all electrodes and membrane were submerged in a solution of 0.5 M NaOH at room temperature to assure the anion conducting sites were in the active form. Testing parameters are listed in **Table 5**, and the list of test iterations is presented in **Table 6**.

Parameter	Constant/Variable
Cell and Feed Temperature	Constant
Feed Stream Flow Rate	Constant
Feed Location (Anode, Cathode, Both)	Variable
Product Pressure	Constant
Feed Stream Composition	Variable
Anode GDL Hydrophobicity	Variable
MEA Preparation Method	Constant

Table 5: Test parameters

Trial #	Hydrophilic Anode GDL				Hydrophobic Anode GDL			
	Inlet H_2O Flow		Inlet K_2CO_3		Inlet H_2O Flow		Inlet H_2O Flow	
	Anode	Cathode	Anode	Cathode	Anode	Cathode	Anode	Cathode
1	X							
2	X	X						
3		X						
4			X					
5			X	X				
6				X				
7		X	X					
8	X			X				
9					X			
10					X	X		
11						X		
12							X	
13							X	X
14								X
15						X	X	
16					X			X

Table 6: List of test iterations

A test protocol was defined prior to beginning testing to keep the resulting data as consistent as possible. This protocol is defined in **Table 7**.

Step	Description	Duration
Break In	Steady State at 200 mA/cm^2	30 minutes
Polarization Curve	Measure potential while varying current from 200 mA/cm^2 to 500 mA/cm^2	10 minutes
Steady State	Steady state at 500 mA/cm^2	4 hours
Polarization Curve	Measure potential while varying current from 200 mA/cm^2 to failure point	10 – 30 minutes
Depolarization	Measure potential with no applied current	At least 5 minutes

Table 7: Test protocol

After bringing the cell and system to temperature, the first step in the protocol was a steady state operation period at low current, which was designed to facilitate catalyst activation and to give the cell a stable charge to begin testing. The following step was a polarization curve to capture a profile of the cell efficiency over a range of input currents up to 500 mA/cm^2. The next step was steady state operation at 500 mA/cm^2, intended to assess stability over time at a current density substantial enough to be a viable system design point. At the end of the steady state period, another polarization curve was collected to compare to the curve collected prior to steady state operation. In this case, the polarization curve was continued beyond 500 mA/cm^2 to a maximum of 1,200 mA/cm^2 or until the cell potential became too high. The data set produced provided a complete profile of a cell's efficiency and stability in the short term for comparison against other cell variations.

Results/Discussion - Inlet Feed Composition

The primary hypothesis entering the study was that doping the inlet stream with K_2CO_3 would result in an improvement in cell efficiency and stability compared with a DI water feed. Results for the anode feed only and dual feed conditions are presented in **Figure 52** as the difference between using a DI water feed and using a K_2CO_3-doped feed in the system.

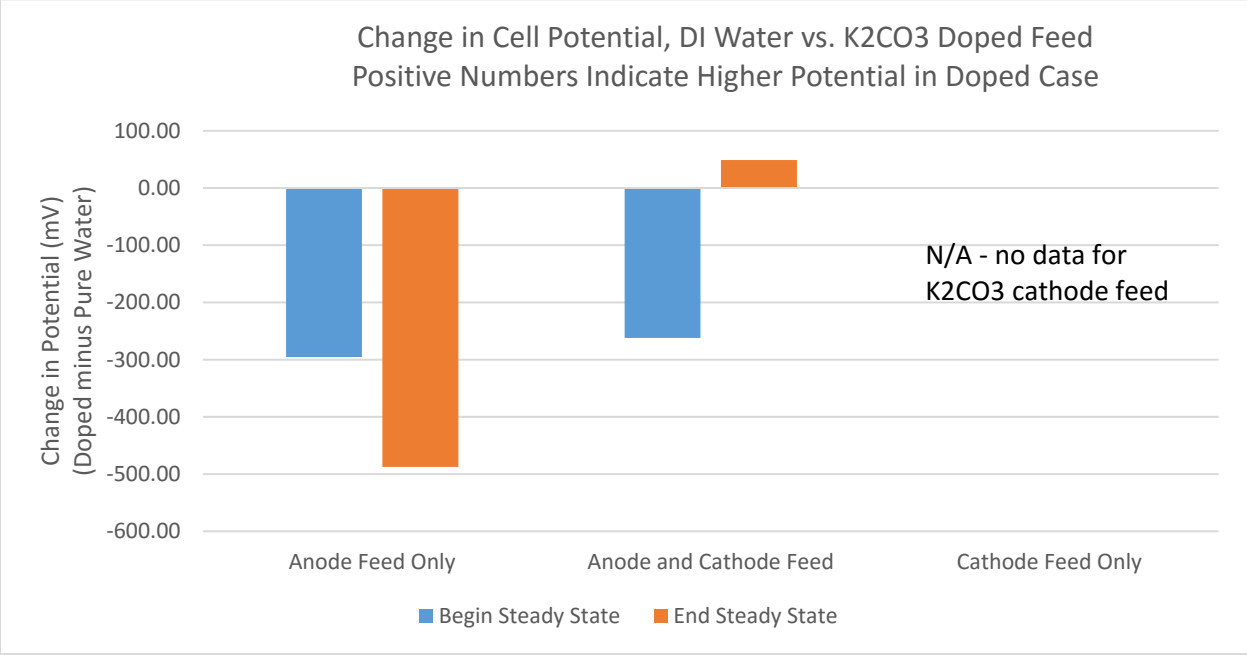

Figure 52: Change in cell potential when doping feed stream with K_2CO_3. Positive change means K_2CO_3 cell had a higher potential. Performance for K_2CO_3 feed to cathode only cell was too poor to complete testing.

In the anode feed only condition, doping the inlet water feed with K_2CO_3 resulted in a substantial improvement in both efficiency and stability of the cell. In the dual feed condition, however, there was an initial improvement in efficiency similar to the improvement in the anode only cell, but over the course of the four hours of steady state operation the performance began to decay more rapidly than in the DI water feed cell. In the cathode feed only configuration, the K_2CO_3-doped cell performed poorly enough that the protocol could not be completed. The positive effect of having a K_2CO_3-doped anode feed was consistent throughout the study, as was the negative effect of having a K_2CO_3-doped feed on the cathode side of the cell.

A complete data set for changes in cell operating potential vs. a water-water dual feed configuration is presented in **Figure 53**.

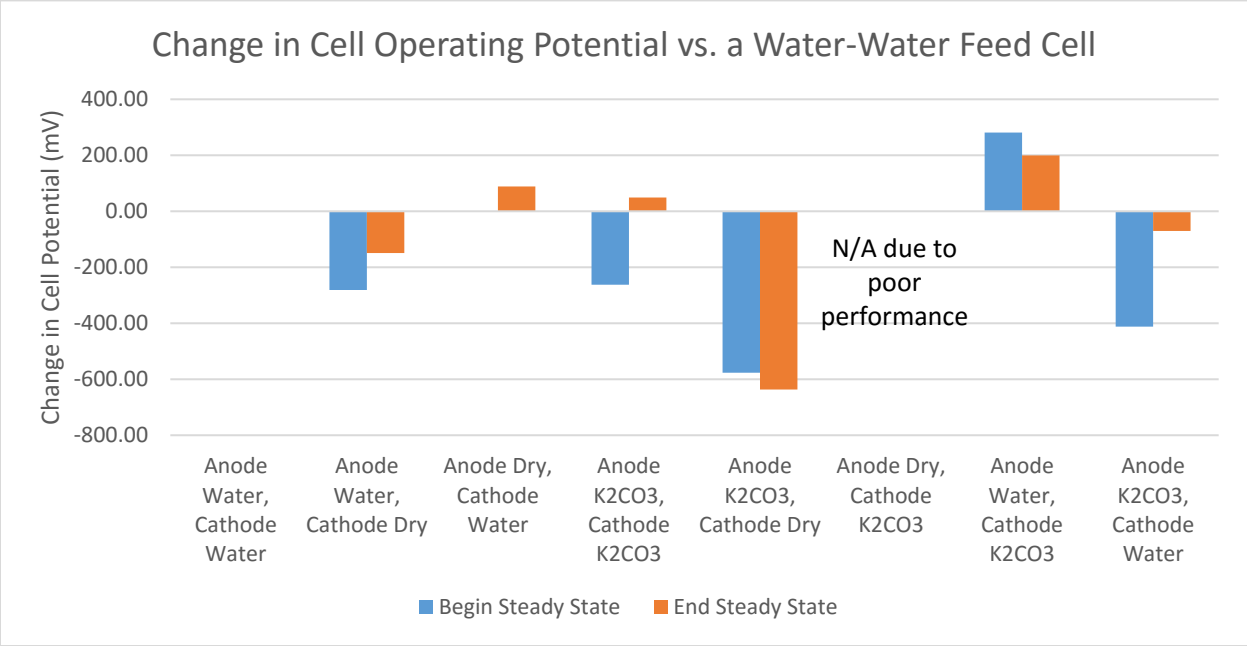

Figure 53: Cell performance vs. dual feed water-water configuration. Positive values represent less efficient cell performance compared to water-water.

Surprisingly, the two best-performing cell configurations were the two configurations with no cathode feed, contrary to the initial theory. The data set in **Figure 53** shows that the improvement from the K_2CO_3 is mitigated by feeding water to the cathode side of the cell, doped or not. The dual feed K_2CO_3 cell and K_2CO_3 anode, water cathode cells each begin the steady state period at a significant improvement over the water-water case, but after four hours show almost no change compared to the water-water case. This effect was repeatable and reproducible, but more analysis and mechanistic study is needed to determine the cause of the instability.

Anode GDL

Figure 54 shows the impact of hydrophobic anode GDLs on cell performance. The impact of using a hydrophobic GDL was considered relatively small. There were several cases where there was a significant difference in cell potential at the beginning of the steady state period, but in all cases the cell potentials trended together and typically ended up being similar. It is likely that, given additional run time, these cases would all have ended up at similar potentials. There seems to be a cell-to-cell variation in charging rate during the initial polarization curves, effectively giving each cell a different starting point in the steady state testing. For this reason, it is considered more useful to look at the cell potential at the end of steady state testing to project long term cell performance. Our conclusion regarding the use of an anode GDL with a hydrophobic treatment is that it does not result in a sustainable change in cell performance. Based on the results of the work conducted in this study, it was decided that the mode of operation was to supply water buffered with carbonate directly to the anode during operation.

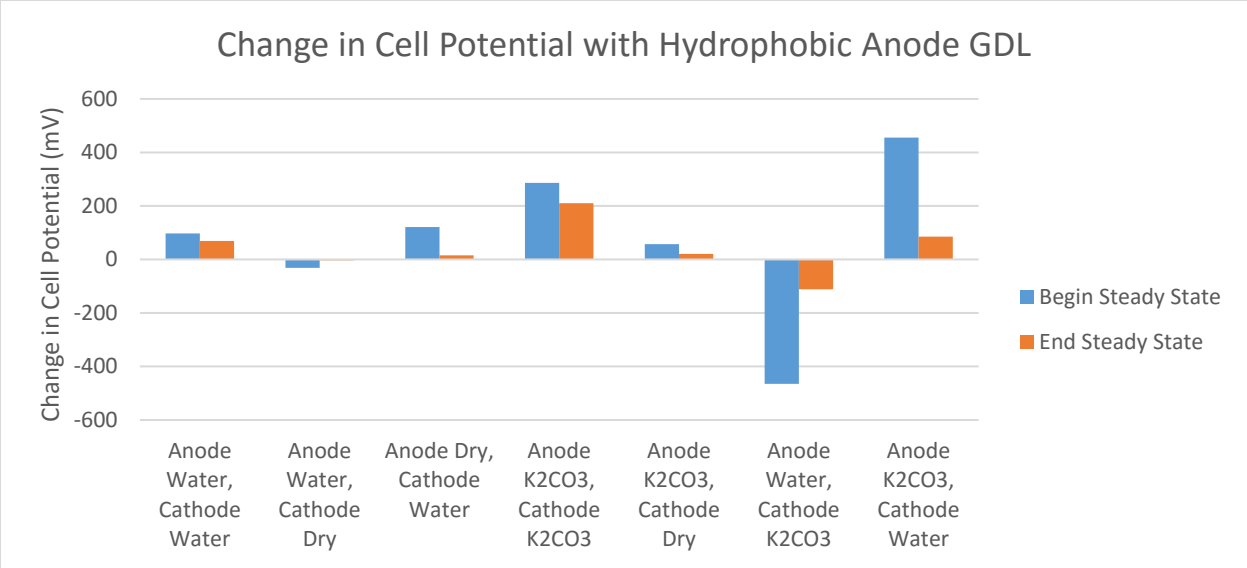

Figure 54: Change in cell potential when using a hydrophobic anode GDL

Final Durability Test

The final durability test stack was assembled as a 3-cell 28 cm^2 stack; a manufacturing issue identified early in the test required removal of one of the cells and the stack was allowed to continue durability testing as a 2-cell stack. The configuration leveraged improvements in cell design to manage the thinner AEM materials available. The test was operated at 50ºC, 50 psi hydrogen generation pressure, 500 mA/cm^2, and with carbonate added to the anode water feed. The selection of the anode fed configuration with carbonate was based on the earlier testing discussed showing optimal performance and best overall stability of voltage. Proton's traditional test stand was used since it provided continuous data acquisition of all operating parameters, including gas cross-over measurements to sense for membrane failure. Electrodes were fully non-PGM based and comprised of the down-selected catalysts from Northeastern University. The compositions used were their NiFe/Raney for OER and NiNx/C for HER. This stack used Proton's commercial production hardware to represent the most realistic operating conditions possible. The final milestone at these operating conditions targeted 500 hrs of operational tests time under these conditions, but as shown in **Figure 55** below, we were able to achieve approximately 1000 hrs, doubling the program requirements. The test results shown below demonstrate successful completion of the end of program milestone.

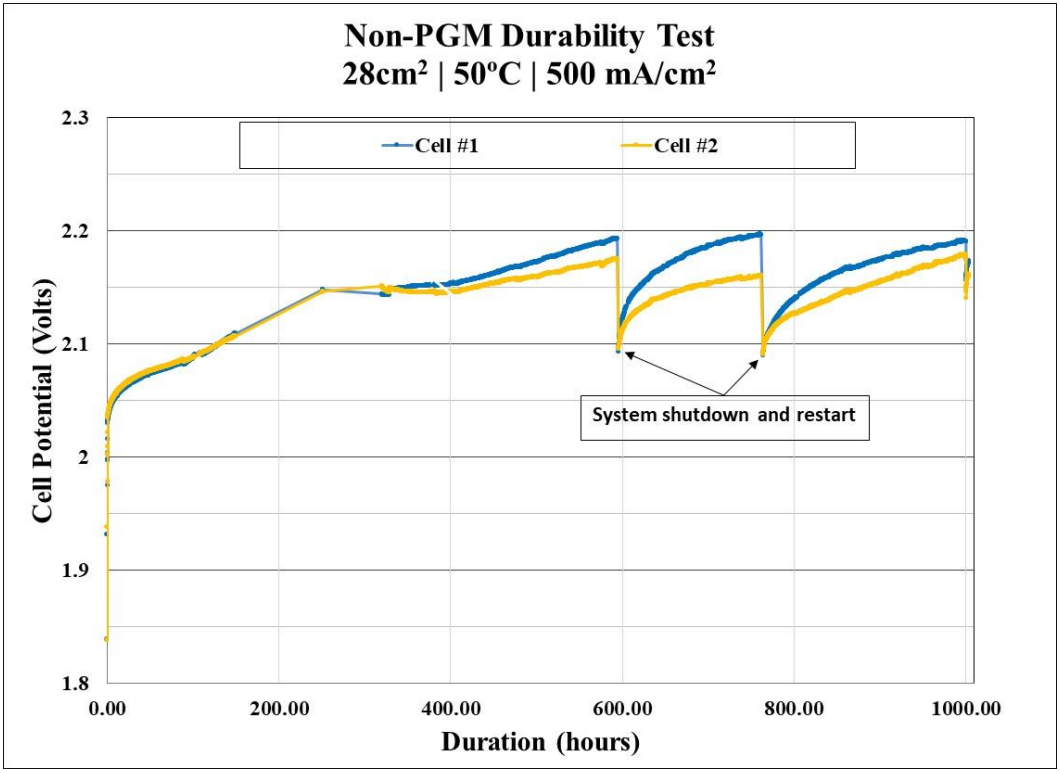

Figure 55: Full non-PGM MEA operated under steady-state conditions for final program milestone

Conclusions and Suggested Future Work:

Over the program duration, there were many advancements realized that have led to significant improvements in multiple areas of AEM water electrolysis. Leveraging the efforts from University partners, we were able to develop non-PGM catalysts, while gaining insights into electrode structure and binder integration when all were incorporated. The non-PGM catalysts developed by Northeastern University use a nickel based composition, which would offer significant material cost reductions versus the PGM materials currently employed by the PEM technology. These catalysts were supplied in scaled-up batches of 15 gram quantities to Proton for ink and electrode development through the creation of a suspension capable of depositing uniform, well-dispersed layers. These formed electrodes were provided to the University of New Mexico in both non-operated and operated conditions for characterization of the physical structure. Analytical techniques developed at the University have shed light on the differences between the Nafion (acid) and AS-4 (alkaline) ionomer when used as a binder. The Nafion appears to have a much better structure with good porosity required for fluid and gas transport within the electrode, while the AS-4 collapses on itself with a reduction in porosity post operation, likely contributing to performance decay when tested in-cell.

Membrane development at Penn State made strides in improving the overall durability of their PPO membrane. Initial findings of chemical attack by solvents used in the electrode fabrication process were addressed through cross-linking of materials. Further improvements in durability were realized when Penn State was put in contact with one of Proton's suppliers and introduced the use of mechanical supports. The work culminated in a new steady-state operational achievement of ~>150hrs.

Ultimately, the final program test demonstrating a full non-PGM, 2-cell stack exceeded the 500 hr target by 2-fold. Collaborative efforts between program partners resulted in the contribution of electrode materials and fundamental analysis that led to a successful test and established new benchmarks for performance and durability in a commercial device.

While significant progress continues to be made, the limiting factor in these devices is still the membrane and ionomer materials and additional research including long term device screening is needed. Suggested work going forward would be to have Penn State look further into degradation mechanisms, improve ionic conduction, and optimize castings around the new mechanical support. Other groups continue to advance different membranes chemistries as well, and the community as a whole should work to drive process. The HydroGEN consortium will likely help with this effort. On the catalyst side, the non-PGM catalysts from Northeastern have shown to be stable during in-cell testing, but their lower activity does incur some performance penalties. Efforts to improve utilization through fabrication refinement and electrode suspensions should be considered. In addition, operating currents >500 mA/cm^2 should be explored. The largest cost savings can be realized through reduction in stack and cell count per system, which can only be achieved by incremental increases in this operating condition.